Electronic Supplementary Material (ESI) for Chemical Science
This journal is © The Royal Society of Chemistry 2013

Fluorinated Diarylamide Complexes of Uranium(III, IV) Incorporating Ancillary Fluorine-to-Uranium Dative Interactions

Haolin Yin, Andrew J. Lewis, Ursula J. Williams, Patrick J. Carroll, and Eric J. Schelter*

P. Roy and Diana T. Vagelos Laboratories, Department of Chemistry, University of Pennsylvania,
Philadelphia, PA 19104

E-mail: schelter@sas.upenn.edu

Supporting Information

Experimental Procedures

General Methods. Unless otherwise indicated all reactions and manipulations were performed under an inert atmosphere (N_2) using standard Schlenk techniques or in a Vacuum Atmospheres, Inc. Nexus II drybox equipped with a molecular sieves 13X / Q5 Cu-0226S catalyst purifier system. Glassware was oven-dried overnight at 150 °C prior to use. ^{1}H, ^{19}F, and ^{13}C NMR spectra were obtained on a Bruker DMX-300 or on a Bruker DMX-360 Fourier transform NMR spectrometer operating at ^{1}H frequency of 300 and 360 MHz, respectively. ^{1}H and ^{19}F variable temperature NMR measurements were carried out at 300MHz and 282 MHz at 300 K (except for VT NMR). Chemical shifts were recorded in units of parts per million referenced against residual proteo solvent peaks (^{1}H) deteuro solvent peaks (^{13}C) or fluorobenzene (^{19}F). Elemental analyses were performed at the University of California, Berkeley, Microanalytical Facility using a Perkin-Elmer Series II 2400 CHNS analyzer. Low resolution mass spectra were collected on a Waters SQD spectrometer using the electro-spray ionization(ESI) technique, operating in negative ion mode. High resolution mass spectrometry (HRMS) data were collected on a Waters LC-TOF mass spectrometer (model LCT-XE Premier) using electrospray ionization (ESI) in positive or negative mode, depending on the analyte. Solution UV-Vis-Near-IR spectra were collected on a PerkinElmer Lambda 950 UV/VIS/NIR Spectrometer at concentrations of ~30 mM. Deconvolution of the f-f transition spectral region was made using fityk.[1] All spectra were successfully fit with a combination of 8 Gaussian functions, including 2 small contributions from an incomplete solvent background correction, indicated by the *'s in Figure S28.

Materials. Tetrahydrofuran, diethyl ether, dichloromethane, fluorobenzene, hexanes, and n-pentane were purchased from Fisher Scientific. The solvents were sparged for 20 min with dry

N_2 and dried using a commercial two-column solvent purification system comprising columns packed with Q5 reactant and neutral alumina respectively (for hexanes and n-pentane), or two columns of neutral alumina (for THF, Et_2O and toluene). Deuterated solvents were purchased from Cambridge Isotope Laboratories, Inc. and stored over potassium mirror overnight prior to use. UI_3 and $UI_4(OEt_2)_4$ were prepared following published procedures.[2] Decafluorodiphenylamine and *N*-phenylpentafluoroaniline were prepared according to reported procedures[3, 4] and purified by sublimation.

X-Ray Crystallography. X-ray reflection intensity data were collected on a Bruker APEXII CCD area detector employing graphite-monochromated Mo-Kα radiation (λ = 0.71073 Å) at a temperature of 143(1) K. In all cases, rotation frames were integrated using SAINT,[5] producing a listing of unaveraged F^2 and $\sigma(F^2)$ values which were then passed to the SHELXTL[6] program package for further processing and structure solution on a Dell Pentium 4 computer. The intensity data were corrected for Lorentz and polarization effects and for absorption using TWINABS[7] or SADABS.[8] The structures were solved by direct methods (SHELXS-97).[9] Refinement was by full-matrix least squares based on F^2 using SHELXL-97.[9] All reflections were used during refinements. The weighting scheme used was $w = 1/[\sigma^2(F_o^2) + (0.0907P)^2 + 0.3133P]$ where $P = (F_o^2 + 2F_c^2)/3$. Non-hydrogen atoms were refined anisotropically and hydrogen atoms were refined using a riding model.

Synthetic Details and Characterization

Synthesis of HNPhAr^F. A Teflon-sealed glass vessel was charged with $Pd_2(dba)_3$ (533 mg, 0.58 mmol, 1.5 mol %), BINAP (1.09 g, 1.75 mmol, 4.5 mol %), and 35 mL of toluene. The slurry was heated at 80 ºC for 20 min with stirring. The resulting red solution was transferred into a glass vessel containing Cs_2CO_3 (19.30 g, 59.24 mmol, 1.53 equiv) and 3,5-bis(trifluoromethyl) bromobenzene (11.36 g, 38.77 mmol, 1.00 equiv) in about 10 mL of toluene under N_2. Aniline (3.62 g, 38.88 mmol, 1.00 equiv) was added and the vessel was sealed under N_2 with a Teflon screw cap. After heating at 100 ºC for 36 h, the mixture was cooled to room temperature, filtered through Celite packed on a coarse porosity fritted filter, and the Celite was rinsed with CH_2Cl_2. Removal of volatiles under reduced pressure yielded an oily red residue, which was purified by chromatography on silica with 1% CH_2Cl_2/hexanes, affording HNPhAr^F as a white crystalline solid. Yield: 9.80 g, 32.11 mmol, 83 %. ^{1}H NMR (benzene-d_6): δ 7.29 (s, 1H), 7.07 (t, 2H, J = 9.0 Hz), 6.92 (s, 2H), 6.85 (t, 1H, J = 9.0 Hz), 6.74 (d, 2H, J = 9.0 Hz), 4.83 (s, 1H). ^{13}C NMR (benzene-d_6): δ 145.9, 140.9, 133.4, 132.9, 130.3, 126.2, 124.2, 122.6, 120.8, 115.6. ^{19}F NMR (benzene-d_6): δ –62.9. ESI-MS (CH_2Cl_2): 304.0 ([NPhAr^F]$^-$). Elemental analysis found (calculated) for $C_{14}H_9F_6N$: C, 55.07 (55.09); H, 3.09 (2.97); N, 4.53 (4.59).

Synthesis of KNPh$^F_2$(Et$_2$O). To a 250 mL Erlenmeyer flask containing HNPh$^F_2$ (8.00 g, 22.9 mmol, 1.00 equiv) dissolved in Et_2O, KH (1.50 g, 37.5 mmol, 1.60 equiv) was slowly added resulting in gas evolution. After stirring for 2 h, the slurry was filtered through Celite packed on a coarse porosity fritted filter and the Celite was washed 3 × 10 mL Et_2O. Removal of volatiles under reduced pressure yielded a white solid, which was dissolved in minimum Et_2O (~25 mL). Storage of the solution at –21 °C for one week resulted in colorless crystals which were collected by filtration on a coarse porosity fritted filter. X-ray structure analysis on the crystalline product

revealed the composition as $KNPh^F_2(Et_2O)$. Yield: 8.33 g, 18.1 mmol, 79 %. ^{19}F NMR (Et_2O): δ –161.39 (dd, 4F, *J* = 21, 12 Hz), –169.53 (t, 4F, *J* = 21 Hz), –183.20 (m, 2F, *p*-F). HRMS (MeCN) observed (calculated) for $[C_{12}NF_{10}]^-$: 347.9862 (347.9871).

Synthesis of KNPhPh^F. To a 500 mL Erlenmeyer flask containing $HNPh^F_2$ (1.30 g, 5.0 mmol, 1.00 equiv) dissolved in 250 mL Et_2O, KH (0.30 g, 0.75 mmol, 1.50 equiv) was slowly added, resulting in gas evolution. After stirring for 2 h, the slurry was filtered through Celite packed on a coarse porosity fritted filter, and the Celite was washed 3 × 5 mL Et_2O. Removal of volatiles under reduced pressure yielded a white solid, which was collected on a fritted filter and the Celite was rinsed with hexanes. Drying under vacuum for 5 h yielded a white powder identified by ^1H NMR as $KNPhPh^F$ with negligible solvation of Et_2O. Yield: 1.35 g, 4.5 mmol, 91 %. ^1H NMR (pyridine-d_5): δ 7.26 (d, 2H, *J* = 7.5 Hz), 7.16 (d, 2H, *J* = 7.5 Hz), 6.66 (t, 1H, *J* = 6.3 Hz, *p*-Ph). ^{19}F NMR (pyridine-d_5): 158.02 (dd, 2F, J_1 = 20.7, J_2 = 12.6 Hz), 170.96 (t, 2F, *J* = 23.3 Hz), 189.93 (m, 1F, *p*-Ph^F). HRMS (MeCN) observed (calculated) for $[C_{12}H_5NF_5]^-$: 258.0340 (258.0342).

Synthesis of KNPhAr^F. To a 125 mL Erlenmeyer flask containing $HNPhAr^F$ (1.51 g, 5.0 mmol, 1.00 equiv) dissolved in 50 mL of Et_2O, KH (0.30 g, 0.75 mmol, 1.50 equiv) was slowly added resulting in gas evolution. After stirring for 2 h, the slurry was filtered through Celite packed on a coarse porosity fritted filter and washed with 3 × 5 mL Et_2O. Removal of volatiles under vacuum yielded a yellow solid, which was collected on a fritted filter and washed with hexanes. Drying under vacuum for 5 h yielded a bright yellow powder identified by ^1H NMR as $KNPhAr^F$ with negligible solvation by Et_2O. Yield: 1.50 g, 4.4 mmol, 87 %. ^1H NMR (pyridine-d_5): δ 7.66 (s, 2H, *o*-Ar^F), 7.54 (d, 2H, *J* = 8.1 Hz, *o*-Ph), 7.30 (t, 2H, *J* = 7.2 Hz, *m*-Ph), 6.77 (t, 1H, *J* = 7.2

Hz, *p*-Ph), 6.73 (s, 1H, p-Ar^F). ^{19}F NMR (pyridine-d_5) δ –62.48 (s, 6F). HRMS (MeCN) observed (calculated) for $[C_{14}H_8NF_6]^-$: 304.0572 (304.0561).

Synthesis of $KNPhAr^F$ $(THF)_{0.5}$. To a vial containing $HNPhAr^F$ (1.49 g, 4.9 mmol, 1.00 equiv) dissolved in THF, solid KH (235 mg, 5.9 mmol, 1.20 equiv) was slowly added resulting in gas evolution and a color change to bright yellow. After stirring for 2 h, the slurry was filtered through Celite packed on a coarse porosity fritted filter, which was further washed with THF. Removal of volatiles under vacuum yielded a yellow solid with tinges of brown, which was washed with n-pentane to afford $KNPhAr^F$ $(THF)_{0.5}$ as a bright yellow powder. Yield: 1.57 g, 4.14 mmol, 85%. The product could be further purified by recrystallization from a concentrated solution in THF layered with hexanes at −21 ºC to yield $KNPhAr^F$ $(THF)_3$ as large yellow blocks.

Synthesis of $KNPh_2$. To a 20 mL vial containing $HNPh_2$ (0.85 g, 5.0 mmol, 1.00 equiv) dissolved in 8 mL Et_2O, an 10 mL Et_2O solution of $KNTMS_2$ (1.00 g, 5 mmol, 1.00 equiv), was added resulting in precipitation of a yellow solid. After stirring for 2 h, the slurry was filtered through fritted filter and the solid was washed with 2 × 5 mL Et_2O. Drying under reduced pressure yielded pale yellow powder identified by ^1H NMR as $KNPh_2$ without solvation. Yield: 0.87 g, 4.2 mmol, 84 %. ^1H NMR (pyridine-d_5): δ 7.50 (d, 4H, J = 9.0 Hz, *o*-Ph), 7.22 (t, 4H, J = 9.0 Hz, *m*-Ph), 6.54 (t, 2H, J = 9.0 Hz, *p*-Ph). HRMS (MeCN) observed (calculated) for $\{[C_{12}H_{10}N]^- + 2H^+\}$: 170.0966 (170.0970). (* compound readily hydrolyzes in the standard HRMS condition).

Synthesis of $U^{IV}(NPh^F_2)_4$. Method A from UI_3. To a vial containing UI_3 (0.080 g, 0.124 mmol, 1.33 equiv) suspended in cold toluene (–21 °C), a cold toluene suspension of $KNPh^F_2(Et_2O)$

(0.13 g, 0.29 mmol, 3.00 equiv) was slowly added. The mixture was exposed to dynamic vacuum while stirring. The solution was pumped down to dryness over 2 h. Hexanes (15 mL) was added and the mixture was filtered through Celite packed into a glass pipette to yield an orange filtrate. The orange hexanes solution was concentrated and stored at –21 °C to obtain red crystals in low yield. Crystals suitable for X-ray structure analysis were obtained in the same manner.

Synthesis of $U^{IV}(NPh^{F}_{2})_4$. Method B from $UI_4(Et_2O)$. To a vial containing $KNPh^{F}_{2}(Et_2O)$ (0.37 g, 0.8 mmol, 4.00 equiv) dissolved in 5 mL Et_2O, an Et_2O solution containing $UI_4(Et_2O)_2$ (0.18 g, 0.2 mmol, 1.00 equiv) was slowly added causing an immediate color change to orange. After stirring for 1 h, the slurry was filtered through Celite packed on a coarse porosity fritted filter and washed with 3 × 5 mL Et_2O. The volatiles were removed under reduced pressure. Hexanes (150 mL) was added and the mixture was filtered through Celite packed on a coarse porosity fritted filter to yield an orange filtrate. The hexanes solution was concentrated to 100 mL and stored at –21 °C to yield red crystals which were collected and dried under reduced pressure. Yield: 0.13 g, 0.077 mmol, 39%. ^{19}F NMR (toluene-d_8): δ –155.97 (t, 4F, *p*-F, J = 21 Hz), –164.34 (m, 8F, *m*-F), –276.77 (br, 8F, FWHM 1.69). Elemental analysis found (calculated) for $C_{48}F_{40}N_4U$: C, 35.05 (35.35); H, 0.3 (0); N, 3.6 (3.44).

Synthesis of $U^{IV}(NPhPh^{F})_4$. To a vial containing $KNPhPh^{F}$ (0.24 g, 0.8 mmol, 4.00 equiv) dissolved in 10 mL Et_2O, an Et_2O solution containing $UI_4(Et_2O)_2$ (0.18 g, 0.2 mmol, 1.00 equiv) was added causing an immediate color change to red. After stirring for 1 h the mixture was filtered through Celite packed on a coarse porosity fritted filter and washed with 3 × 5 mL Et_2O. The volatiles were removed under reduced pressure. Hexanes (40 mL) were added to extract the product and the mixture was filtered through Celite packed on a coarse porosity fritted filter to

yield a red filtrate. The hexanes solution was concentrated to 20 mL and stored at –21 °C producing dark red needles which were collected and dried under reduced pressure. Yield: 0.15 g, 0.11 mmol, 59 %. Crystals suitable for X-ray structure analysis were obtained in the same manner but not dried. ^{1}H NMR (toluene-d_8): δ 7.45 (s, 8H), 7.25 (s, 8H), 5.07 (t, 4H, *p*-H, J = 7.5 Hz). ^{19}F NMR (toluene-d_8): δ –167.09 (d, 8F, *m*-F, J = 18 Hz), –168.20 (t, 4F, *p*-F, J = 23 Hz), –303.28 (br, 8F, *o*-F, FWHM 1.11). Elemental analysis found (calculated) for $C_{48}H_{20}N_4F_{20}U$: C, 45.18 (45.37); H, 1.86 (1.59); N, 4.4 (4.41).

Synthesis of $U^{IV}(NPh_2)_4$. $U(NPh_2)_4$ was synthesized according to the reported procedure.[10] An alternative method, as follows, was also developed. To a 20 mL scintillation vial containing $KNPh_2$ (0.17 g, 0.8 mmol, 4.00 equiv) suspended in 10 mL Et_2O, an Et_2O solution containing $UI_4(Et_2O)_2$ (0.18 g, 0.2 mmol, 1.00 equiv) was added causing an immediate color change to red. After stirring for 1 h the mixture was filtered through Celite packed on a coarse porosity fritted filter and washed with 3 × 5 mL Et_2O. The volatiles were removed under reduced pressure. Hexanes (40 mL) was added and the mixture was heated to help extraction. The solution was filtered through Celite packed on a coarse porosity fritted filter to yield a red filtrate. The hexanes solution was concentrated to 30 mL and stored at –21 °C to yield dark red crystals which were collected and dried under vacuum. Yield: 0.080 g, 0.11 mmol, 55 %. The ^{1}H NMR in C_6D_6 was consistent with the reported spectrum.[10]

Synthesis of $U^{IV}(NPhAr^F)_4$. To a 20 mL scintillation vial containing $KNPhAr^F$ (0.28 g, 0.8 mmol, 4.00 equiv) dissolved in 10 mL Et_2O, an Et_2O solution containing $UI_4(Et_2O)_2$ (0.18 g, 0.2 mmol, 1.00 equiv) was added causing an immediate color change to red. After stirring for 1 h the mixture was filtered through Celite packed on a coarse porosity fritted filter and washed with 3 × 5 mL Et_2O. The volatiles were removed under reduced pressure. Hexanes (20 mL) were added

and the mixture was gently heated to help extraction from a black solid. The mixture was filtered through Celite packed into a glass pipette to yield a red filtrate. The hexanes solution was concentrated and stored at –21 °C to yield a dark red amorphous solid which was collected and dried under reduced pressure. Yield: 0.080 g, 0.068 mmol, 34 %. ^{1}H NMR (benzene-d_6): δ 21.10 (s, 8H), 9.10 (s, 4H, *p*-Ar^{F}), –0.39 (s, 8H), –1.53 (t, 4H, *p*-Ph, J = 7.5 Hz), –15.09 (s, 8H). ^{19}F NMR (benzene-d_8): δ –61.20 (s, 24F). Elemental analysis found (calculated) for $C_{56}H_{32}F_{24}N_4U$: C, 46.32 (46.23); H, 2.35 (2.22); N, 3.80 (3.85).

Synthesis of $U^{III}(NPhAr^{F})_3(OPPh_3)_2$. To a dark blue stirring slurry of UI_3 (190 mg, 0.31 mmol 1.00 equiv) in 5 mL THF in a 20 mL scintillation vial, triphenylphosphine oxide (171 mg, 0.61 mmol, 2.00 equiv) was added, causing an immediate color change to dark purple and complete dissolution of residual solid. After cooling this solution to –21 ^{o}C, KNPhAr^{F} $(THF)_{0.5}$ (350 mg, 0.92 mmol, 3.00 equiv) dissolved in about 6 mL THF cooled to –21 ^{o}C was added dropwise. The mixture was allowed to warm to room temperature while stirring for one hour, then cooled to –21 °C to precipitate KI. Filtration through Celite packed on a coarse porosity fritted filter followed by washing with Et_2O yielded a black filtrate. Volatiles were removed under reduced pressure, and the resulting black solid residue was dissolved in about 10 mL of toluene and filtered through Celite suspended in a glass pipette. This solution was concentrated to ~3 mL and layered with ~13 mL of n-pentane and stored at –21 °C, leading to the growth of clusters of black crystalline needles over 2 d. Crystals were isolated on a medium porosity fritted filter, washed with ~25 mL n-pentane, and dried. Yield: 0.399 g, 0.23 mmol, 76%. X-ray structural analysis was performed on a crystal grown in the above manner but not dried. ^{1}H NMR (benzene-d_6): δ 18.33 (s, 12H, *PPh*$_3$), 8.86 (s, 12H, *PPh*$_3$), 8.72 (s, 6H), 3.71 (s, 3H), 2.68 (s, 6H), 2.27 (s, 3H), –4.72 (s, 6H), –7.19 (s, 6H). ^{19}F NMR (benzene-d_6): δ –66.5 (s, 18F). ^{31}P

NMR (benzene-d_6): 266.2 (s, 2P) Elemental analysis found (calculated) for $C_{78}H_{54}F_{18}N_3O_2P_2U\cdot1.5C_7H_8$: C, 57.76 (57.60); H, 3.88 (3.60); N, 2.50 (2.28).

Synthesis of $U^{III}(NPh^F{}_2)_3(THF)_2$. To a 20 mL scintillation vial containing $HNPh^F{}_2$ (1.50g, 4.30 mmol, 3 equiv) dissolved in 10 mL THF, slowly added KH (0.344 g, 8.60 mmol, 6.00 equiv), resulting in bubbling. After stirring for 1 h, the slurry was filtered through Celite suspended in a glass pipette, which was further washed with Et_2O. The filtrate was cooled to −21 °C and a THF solution of UI_3 (0.887 g, 1.43 mmol, 1.00 equiv) was added, causing an immediate color change to purple. After stirring for 1 h allowing the solution to warm to room temperature, the mixture was filtered through Celite packed on a coarse porosity fritted filter. After removal of volatiles under reduced pressure (carefully, to avoid desolvation of the product), 200 mL of hexanes was added and mixture was filtered through Celite packed on a coarse porosity fritted filter. The purple solution was concentrated and stored at –21 °C to yield dark red crystals which were collected and dried under vacuum. Yield: 0.387 g, 0.53 mmol, 37%. Crystals suitable for X-ray analysis were obtained in the same manner but not dried. . ^{19}F NMR (THF): δ –168.33 (d, 12F, *m*-F, *J* = 21 Hz), –174.23 (t, 6F, *p*-F, *J* = 22 Hz), –302.80 (br, 12F, *o*-F, FWHM 1.76). Elemental analysis found (calculated) for $C_{44}H_{16}N_3O_2F_{30}U$: C, 37.21 (37.05); H, 1.50 (1.13); N, 2.90 (2.95).

X-ray Crystal Structures

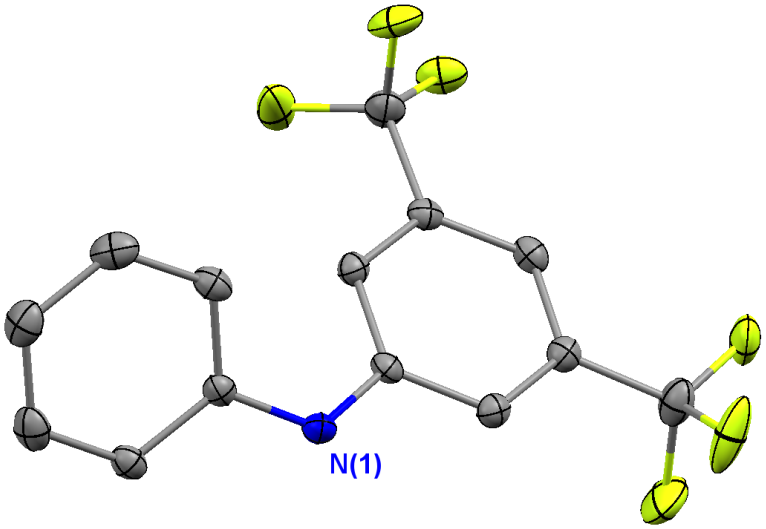

Figure S1. Thermal ellipsoid plot of **HNPhAr^F** at 30% probability. Hydrogen atoms are omitted for clarity.

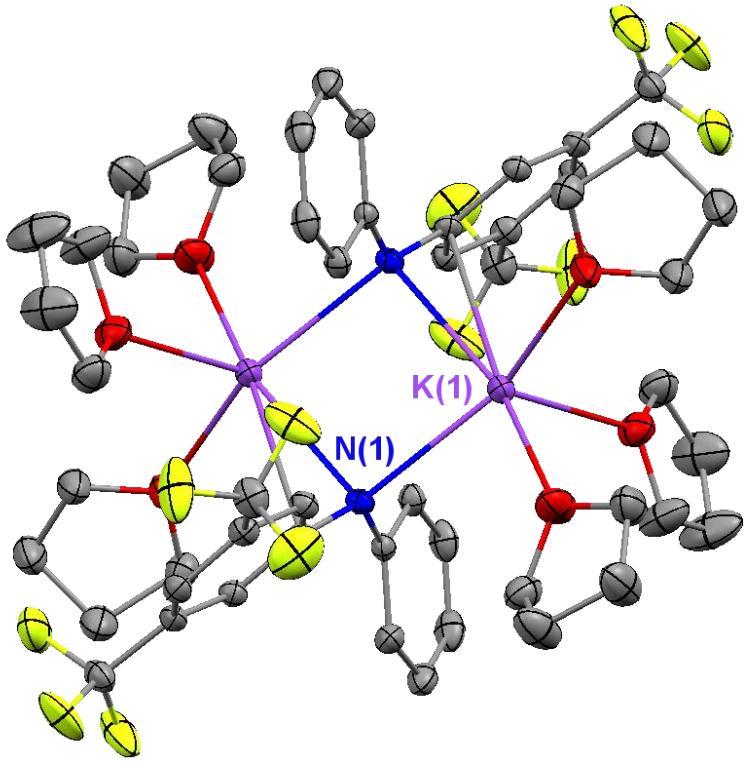

Figure S2. Thermal ellipsoid plot of [**KNPhAr^F(THF)$_3$**]$_2$ at 30% probability. Hydrogen atoms are omitted for clarity

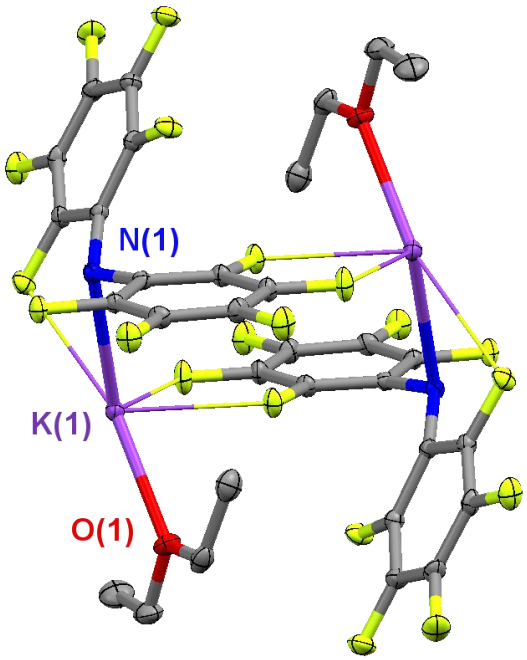

Figure S3. Thermal ellipsoid plot of **KNPh$^F_2$(Et$_2$O)** at 30% probability. Hydrogen atoms are omitted for clarity.

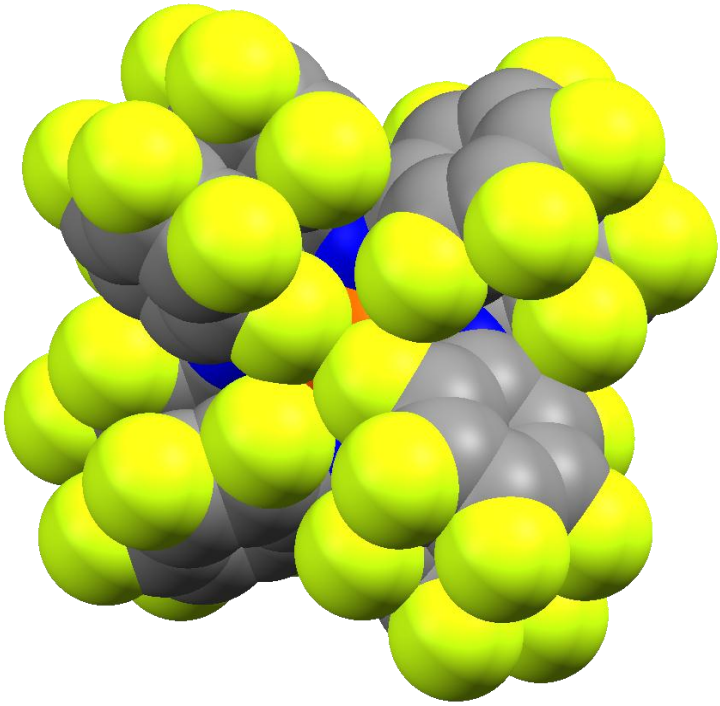

Figure S4 Space-filling diagram of **1-Ph$^F_2$**, emphasizing the collective π-π stacking of the Ph^F rings.

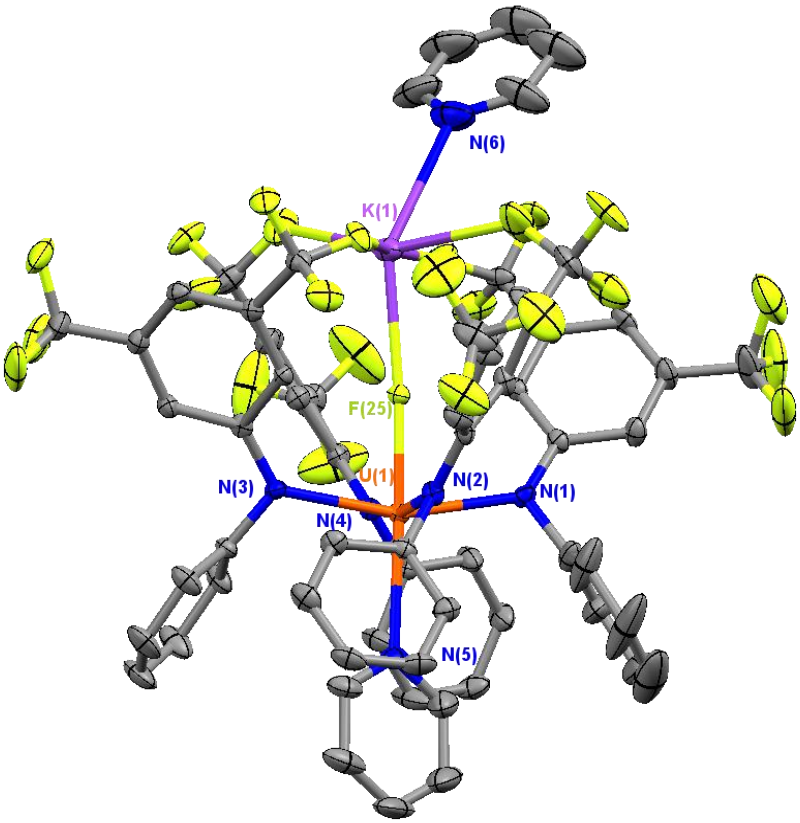

Figure S5. Thermal ellipsoid plot of **[K(py)][U^{IV}(F)(NPhAr^{F})$_4$(py)]** at 30% probability. Hydrogen atoms are omitted for clarity. Selected bond length (Å): U(1)−F(25) 2.143(3), U(1)−N(1) 2.402(4), U(1)−N(2) 2.385(4), U(1)−N(3) 2.351(4), U(1)−N(4) 2.382(4), U(1)−N(5) 2.630(4).

NMR Spectra

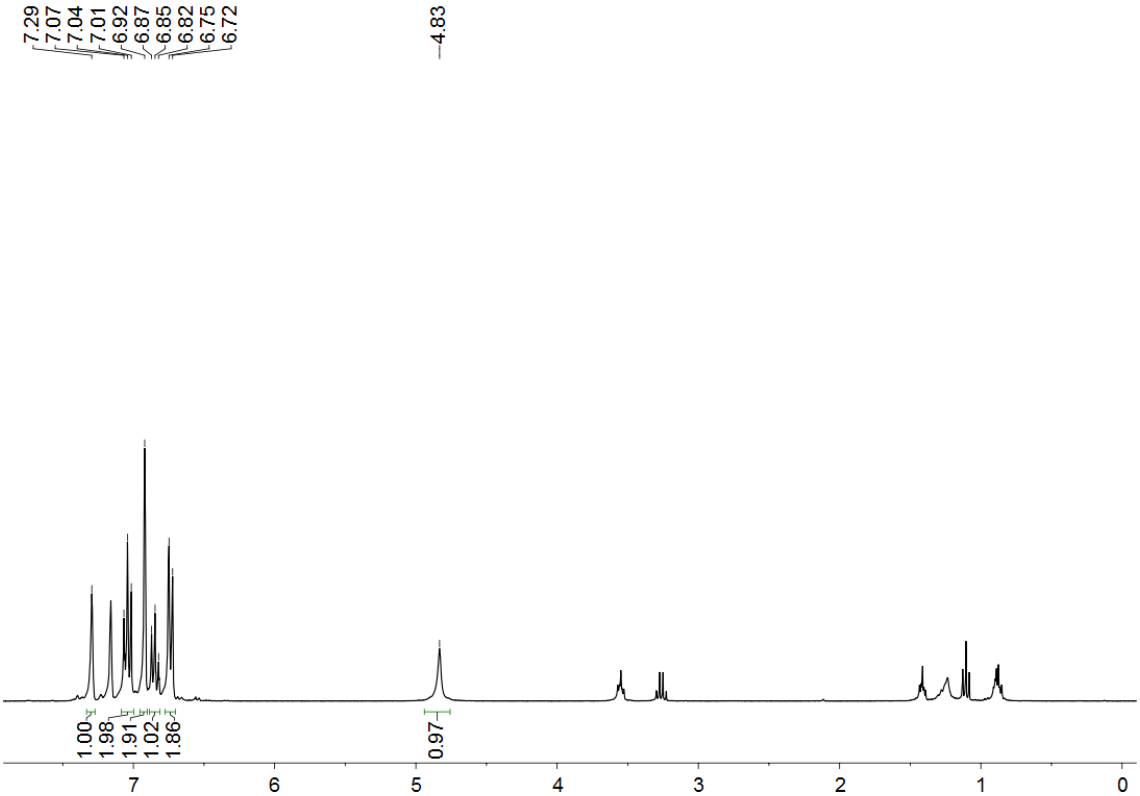

Figure S6. ^{1}H NMR of **HNPhAr^{F}** in benzene-d_6.

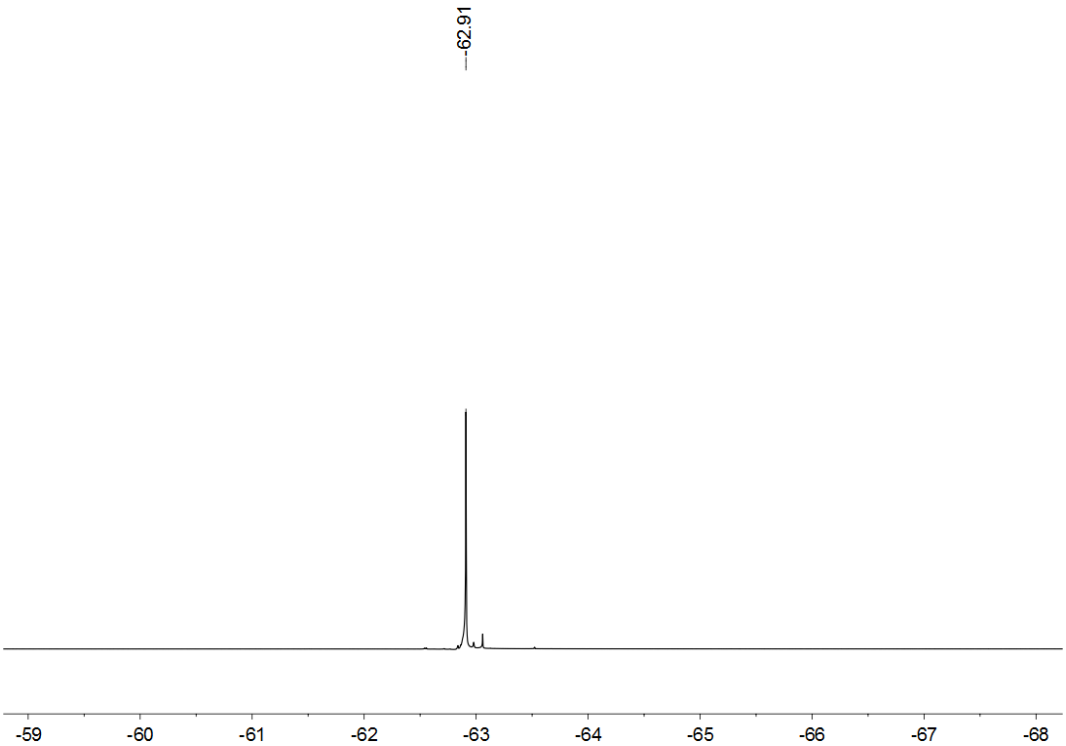

Figure S7. ^{19}F NMR of **HNPhAr^{F}** in benzene-d_6.

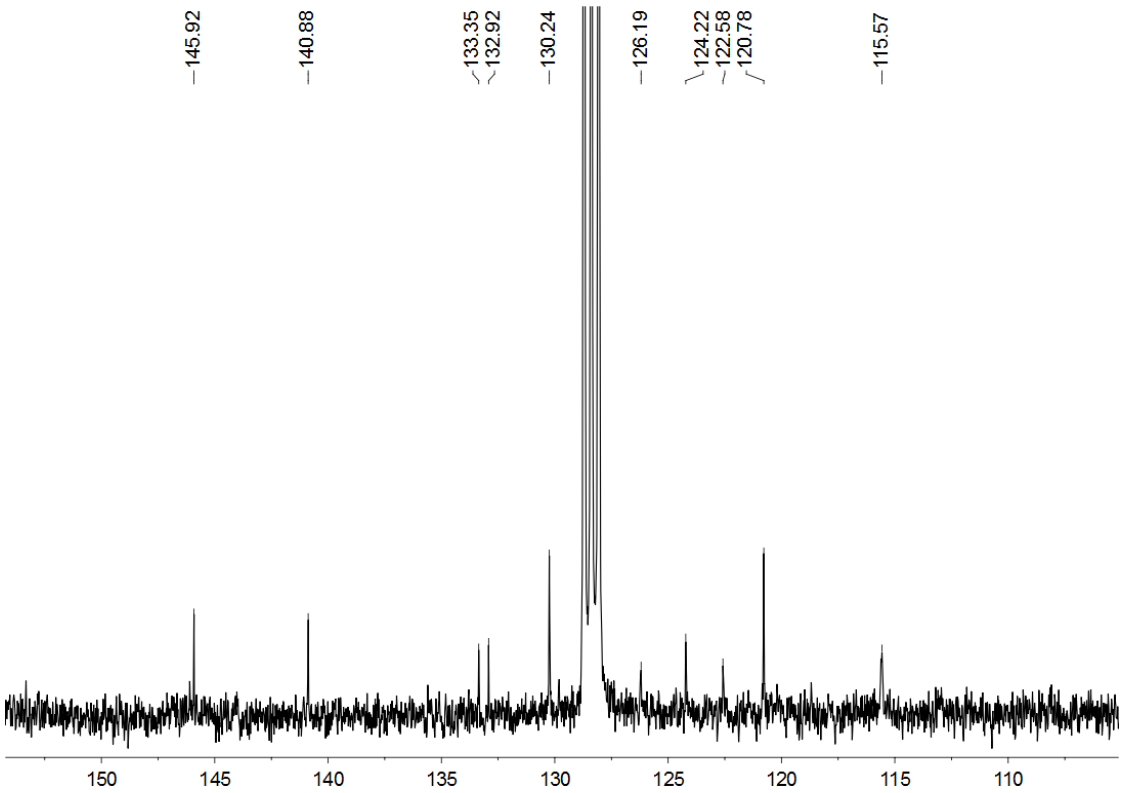

Figure S8. ^{13}C NMR of **HNPhAr^{F}** in benzene-d_6.

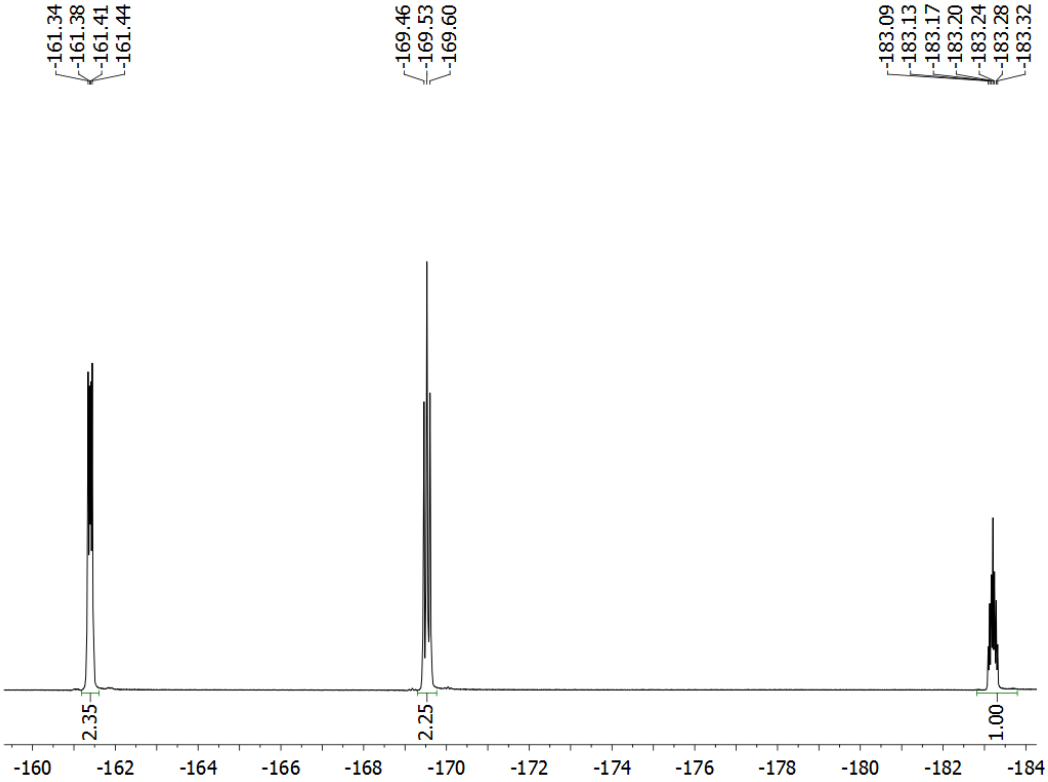

Figure S9. ^{19}F NMR of **KNPh$^{F}_2$(Et$_2$O)** in Et$_2$O.

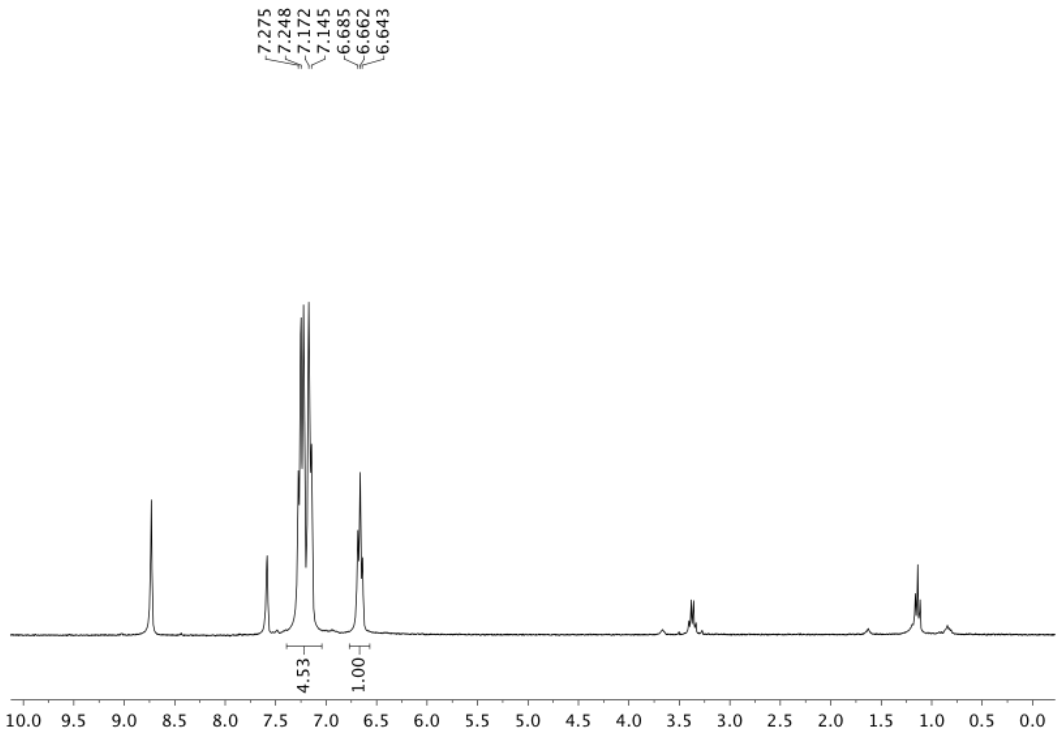

Figure S10. ^{1}H NMR of **KNPhPh^{F}** in pyridine-d_5.

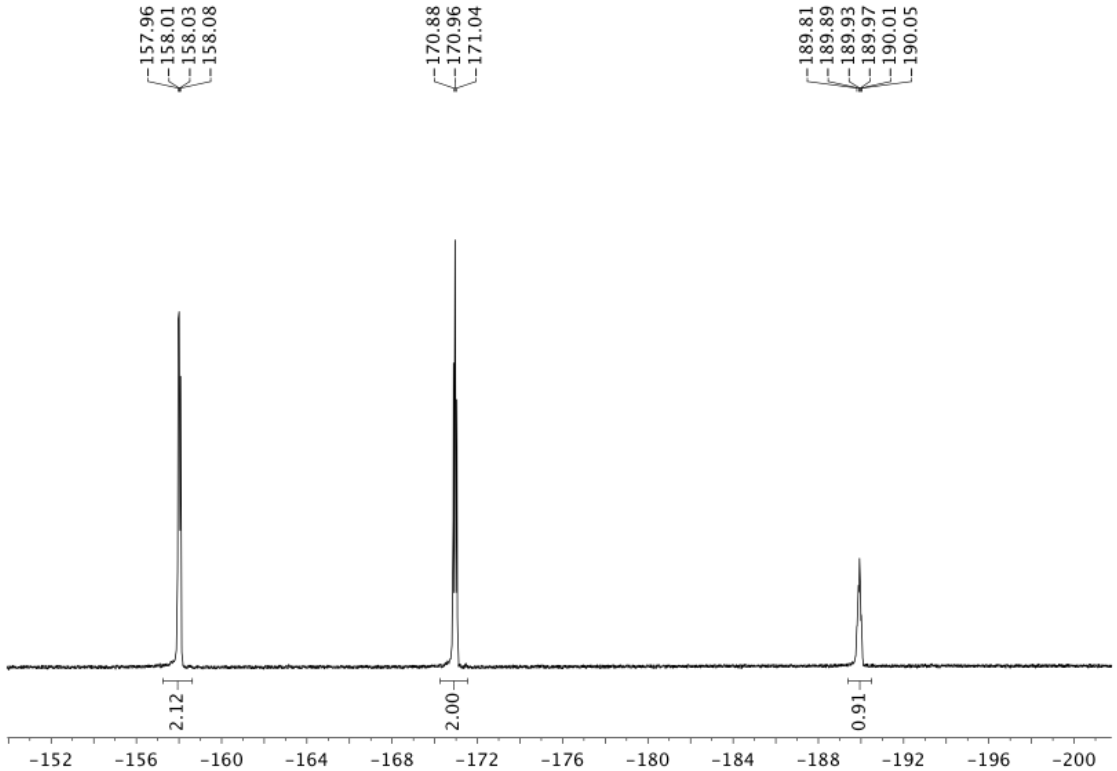

Figure S11. ^{19}F NMR of **KNPhPh^{F}** in pyridine-d_5.

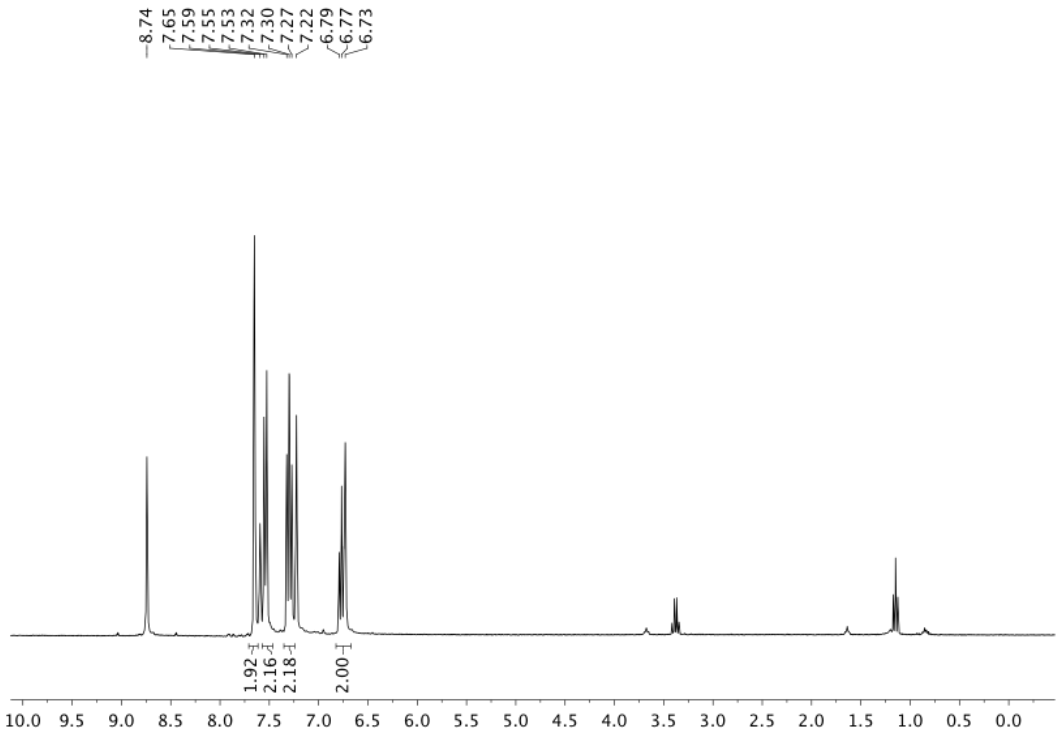

Figure S12. ^{1}H NMR of **KNPhAr^{F}** in pyridine-d_5.

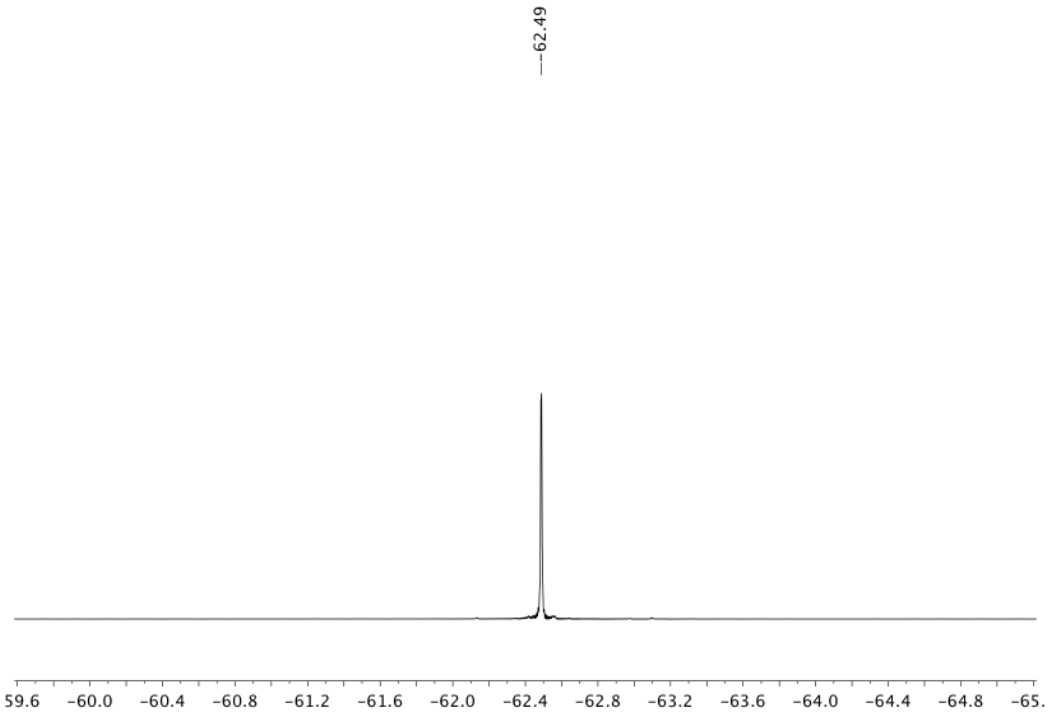

Figure S13. ^{19}F NMR of **KNPhAr^{F}** in pyridine-d_5.

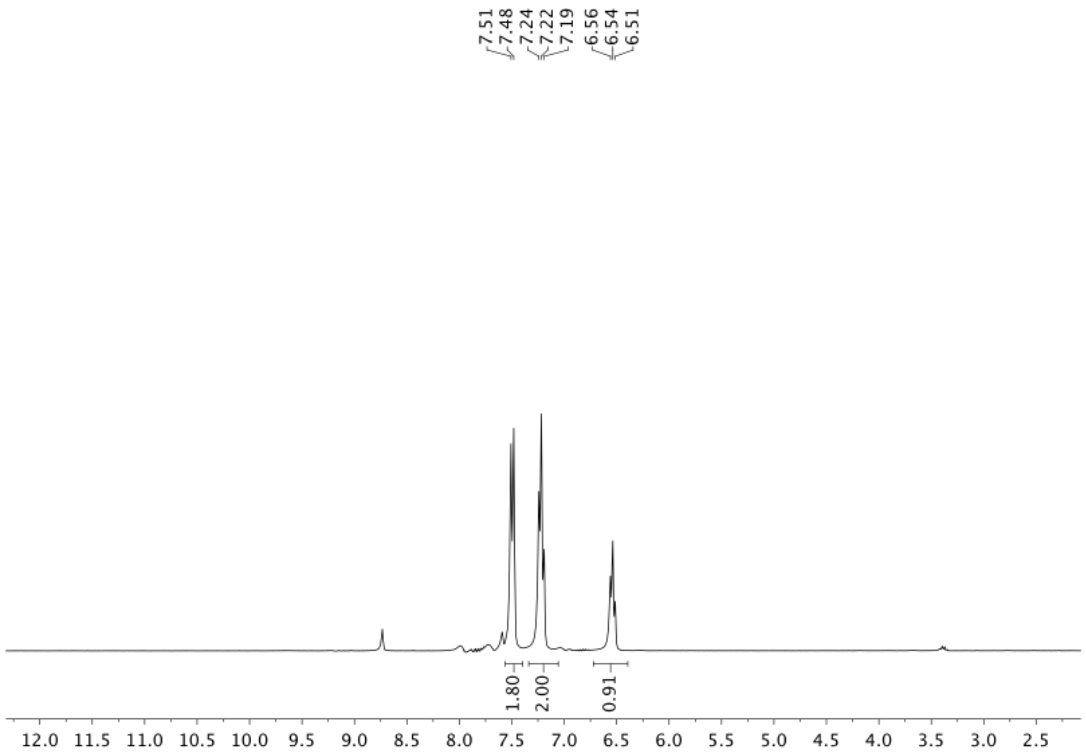

Figure S14. ^{1}H NMR of **KNPh$_2$** in pyridine-d_5.

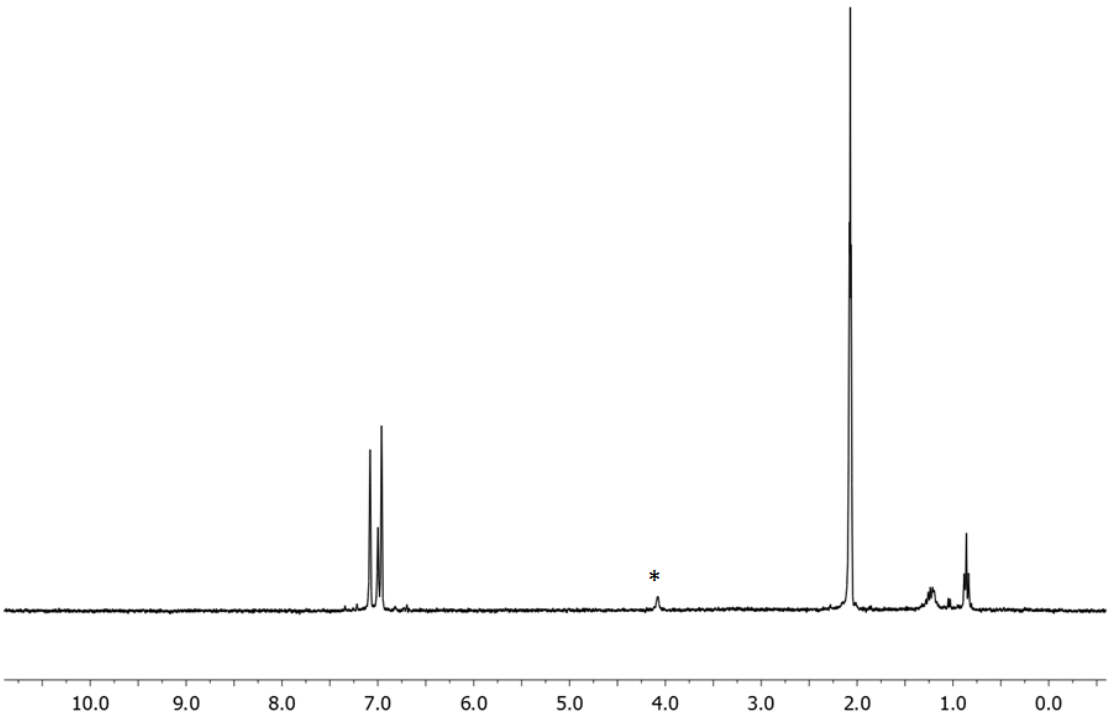

Figure S15. ^{1}H NMR of **U^{IV}(NPh$^{F}_{2}$)$_4$** in toluene-d_8. No peaks are observed except for solvent residue, hexanes and HNPh$^{F}_{2}$ as minor impurity (*).

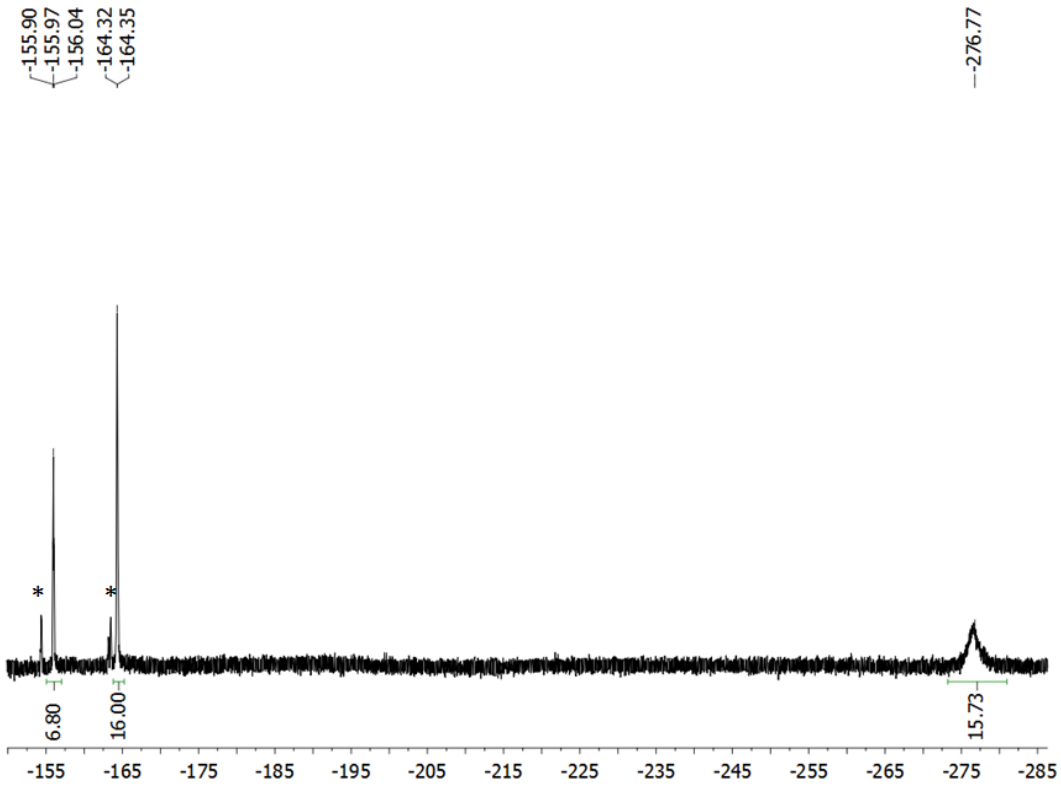

Figure S16. ^{19}F NMR of $\mathbf{U^{IV}(NPh^{F}_{2})_4}$ in toluene-d_8. $HNPh^{F}_{2}$ is noted (*) as a minor impurity.

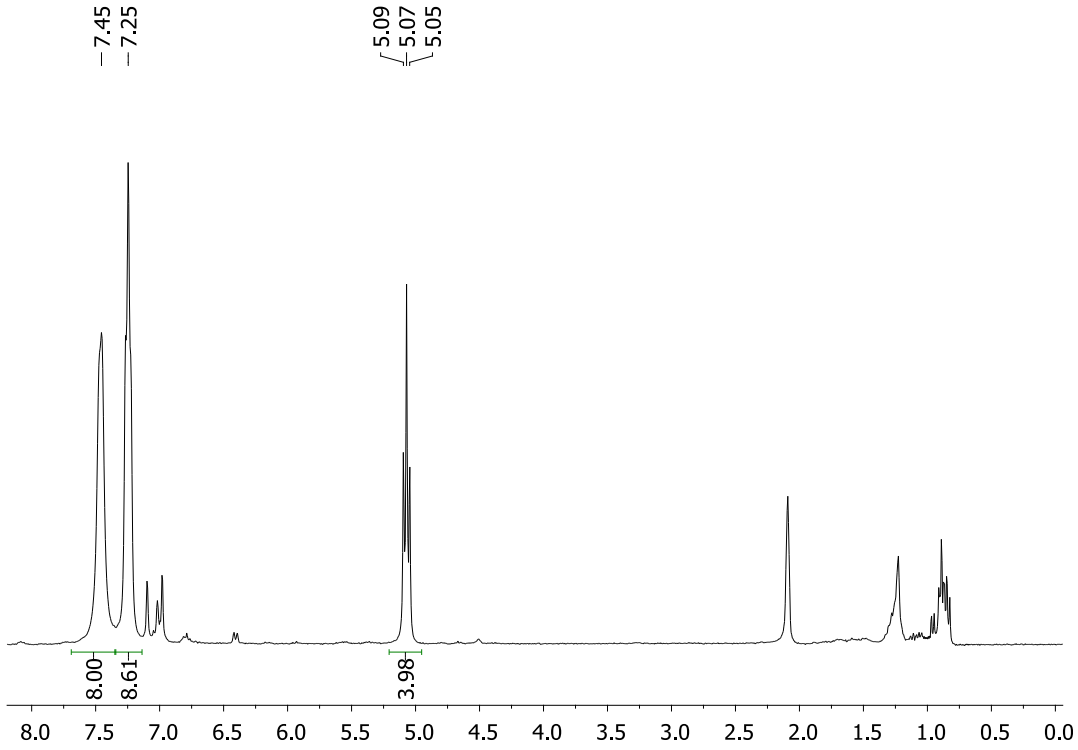

Figure S17. ^{1}H NMR of $\mathbf{U^{IV}(NPhPh^{F})_4}$ in toluene-d_8.

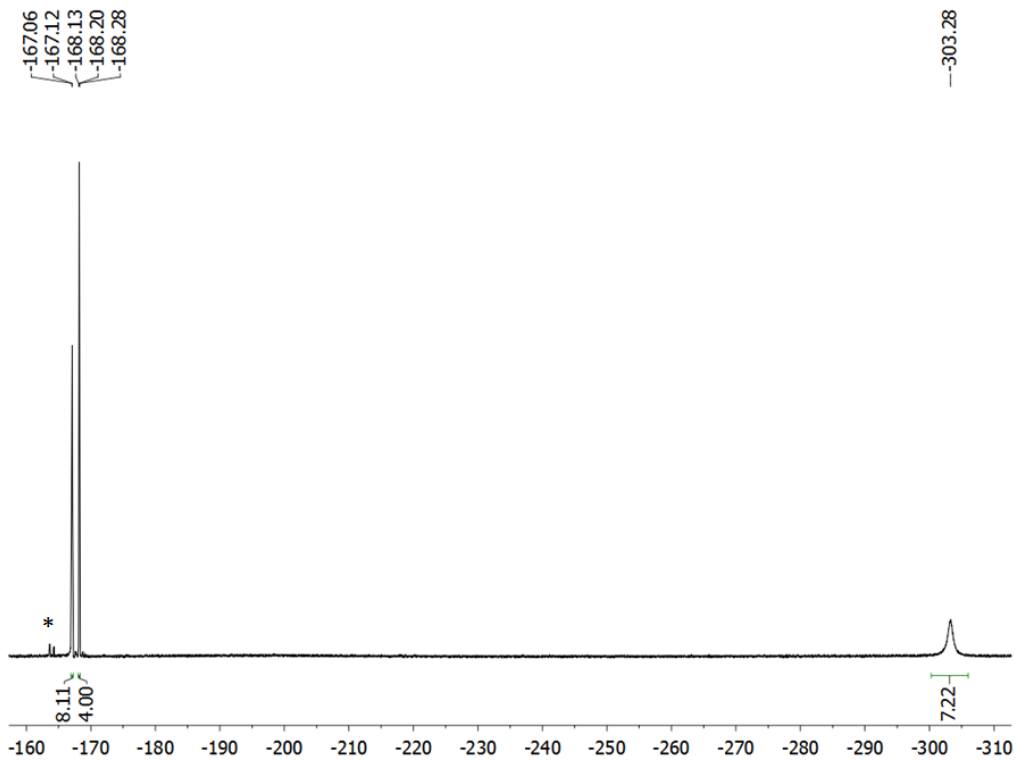

Figure S18. ^{19}F NMR of $\mathbf{U^{IV}(NPhPh^{F})_4}$ in toluene-d_8. HNPhPh^{F} is noted (*) as a minor impurity.

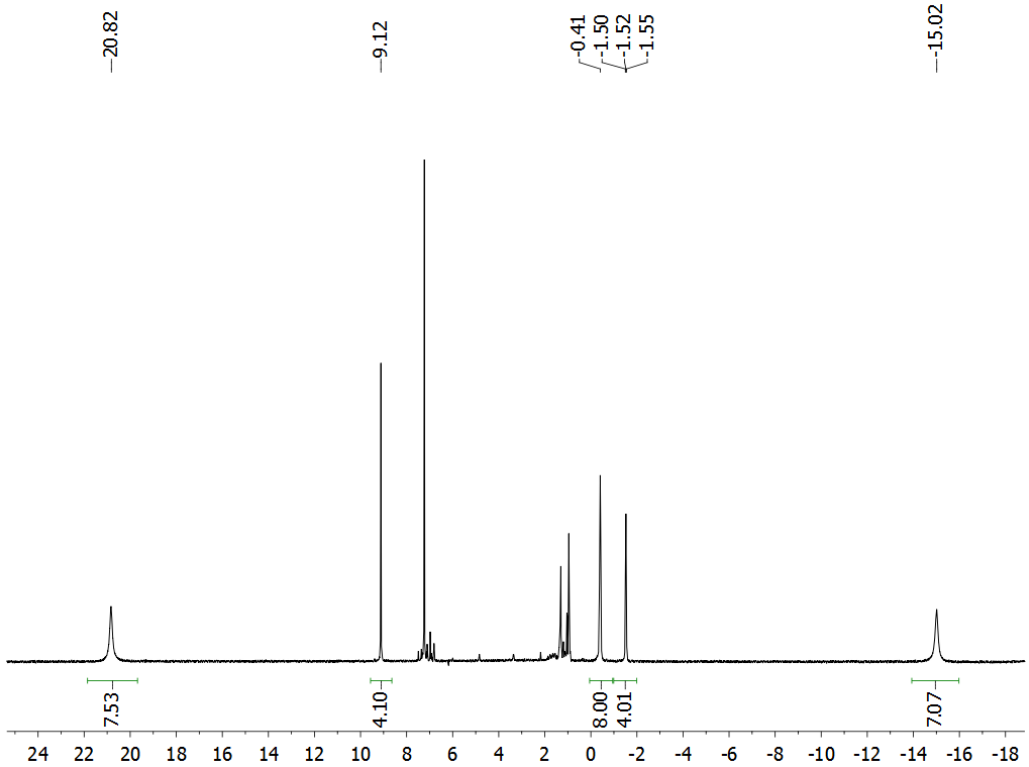

Figure S19. ^{1}H NMR of $\mathbf{U^{IV}(NPhAr^{F})_4}$ in benzene-d_6.

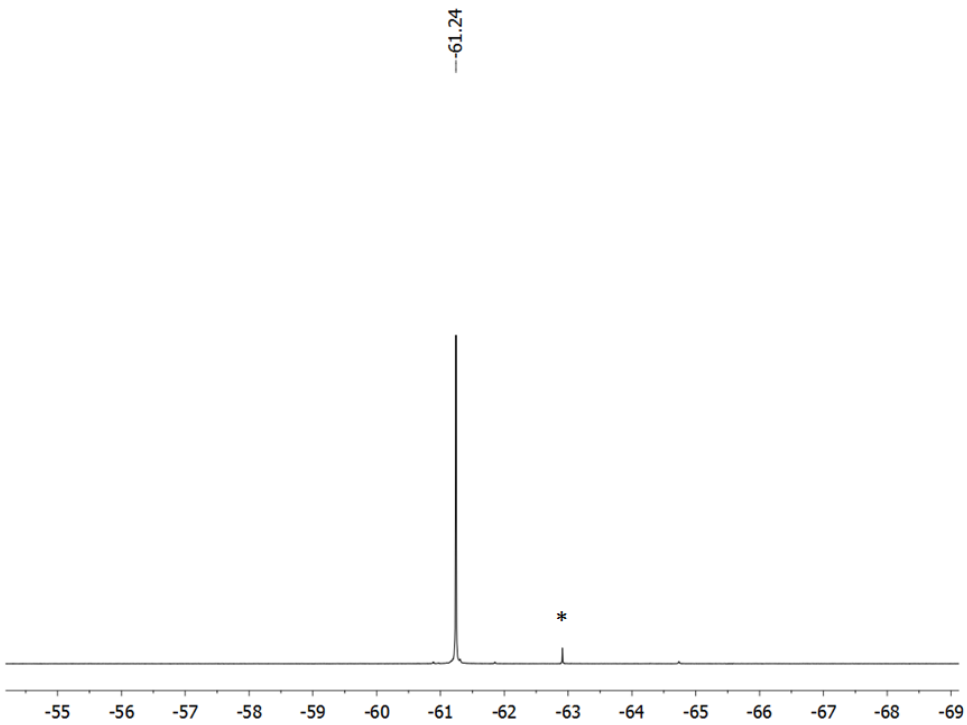

Figure S20. ^{19}F NMR of $\mathbf{U^{IV}(NPhAr^{F})_4}$ in benzene-d_6. HNPhAr^{F} is noted (*) as a minor impurity.

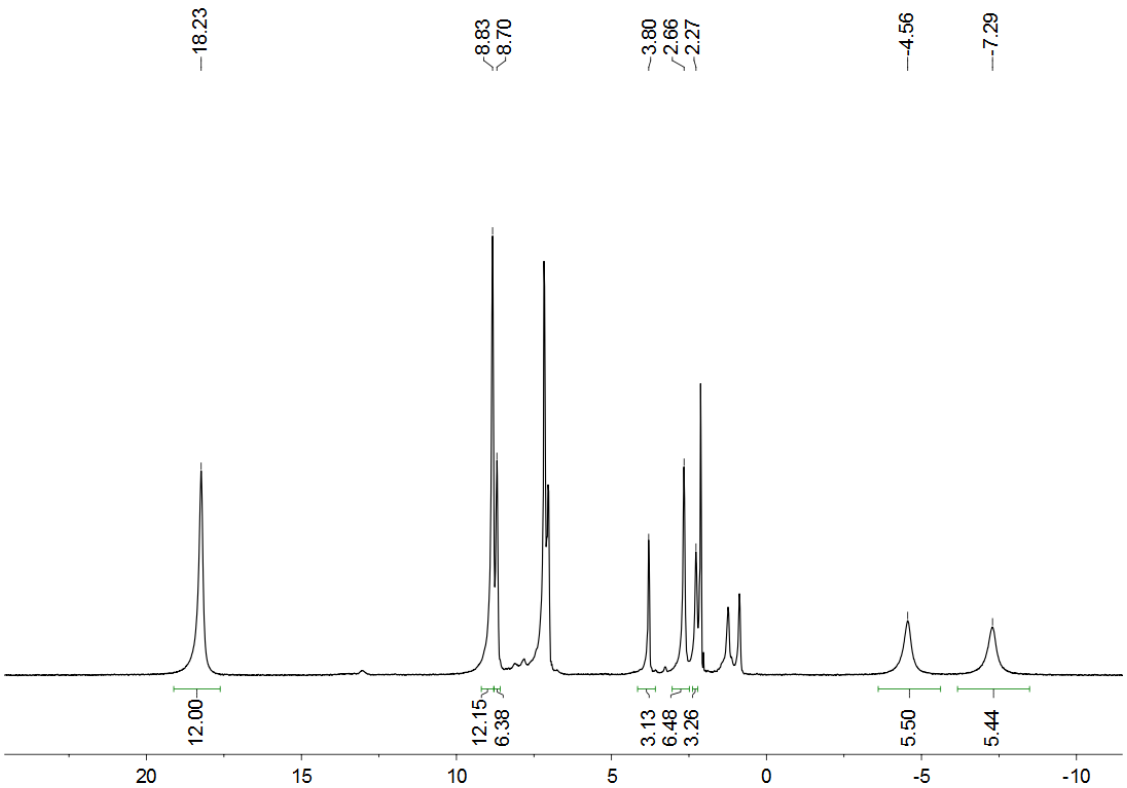

Figure S21. ^{1}H NMR of $\mathbf{U^{III}(NPhAr^{F})_3(OPPh_3)_2}$ in benzene-d_6.

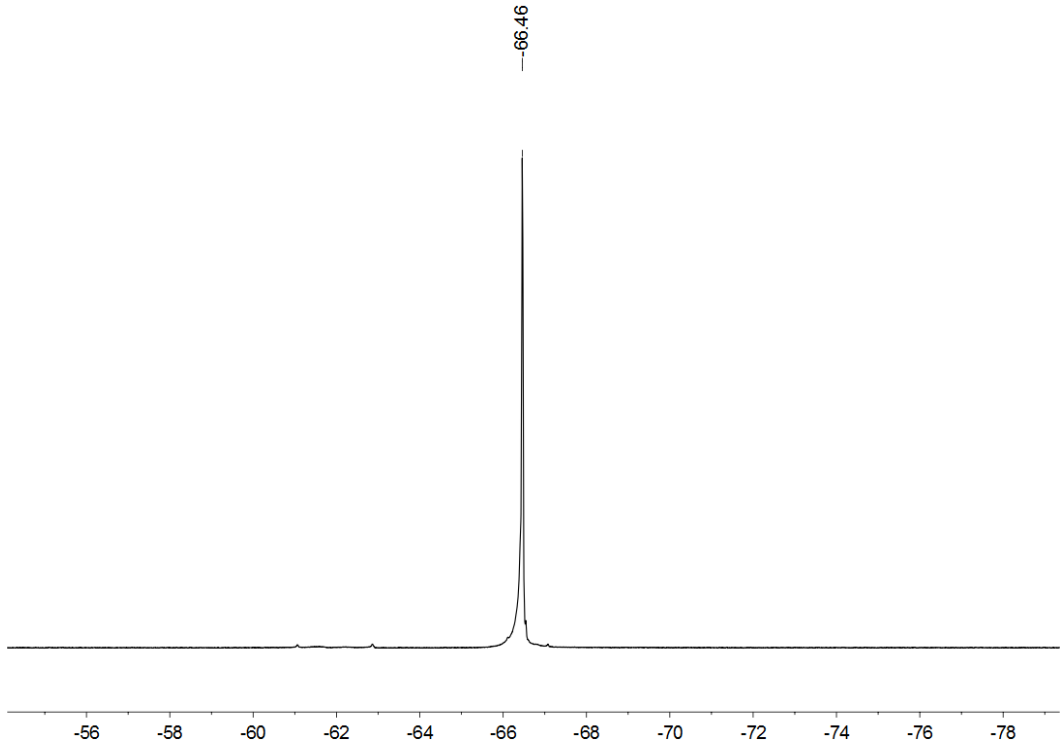

Figure S22. ^{19}F NMR of $\mathbf{U^{III}(NPhAr^{F})_3(OPPh_3)_2}$ in benzene-d_6.

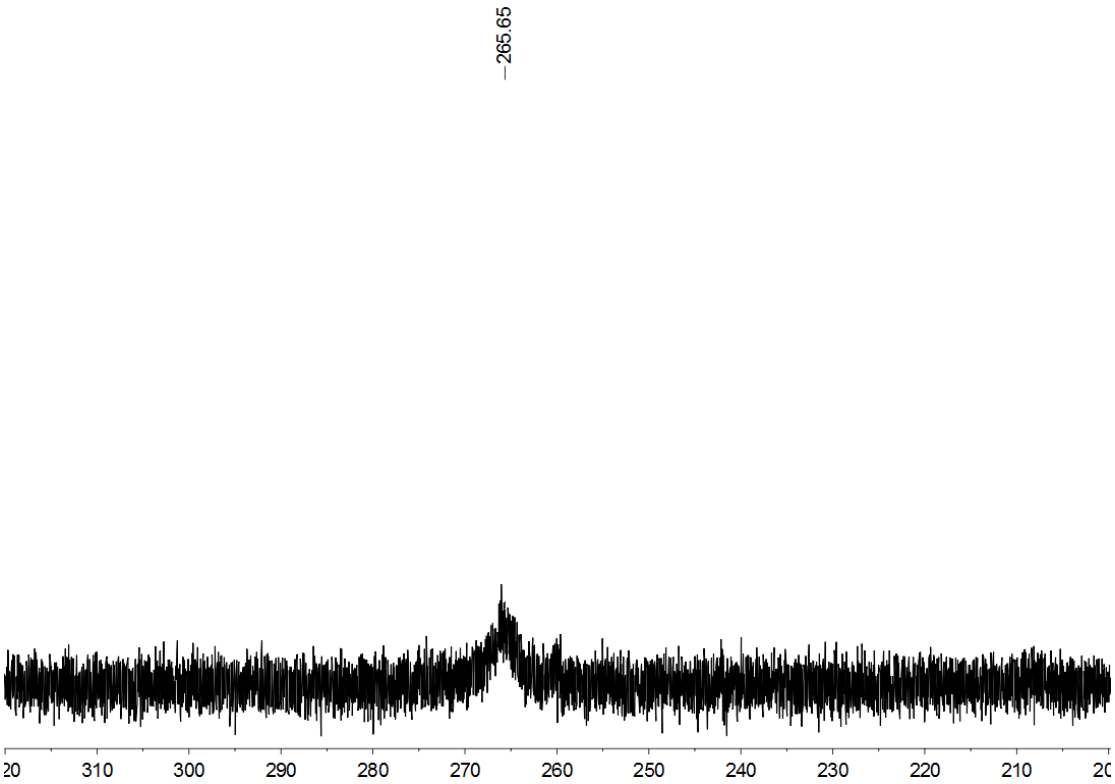

Figure S23. ^{31}P NMR of $\mathbf{U^{III}(NPhAr^{F})_3(OPPh_3)_2}$ in benzene-d_6.

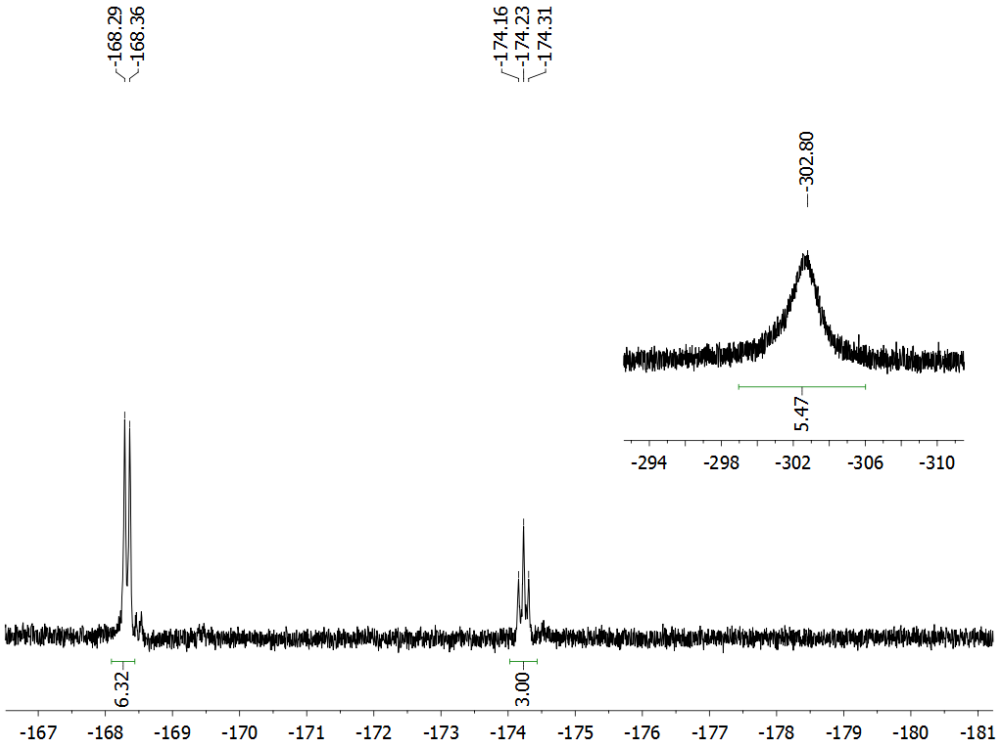

Figure S24. ^{19}F NMR of $\mathbf{U^{III}(NPh^{F}_{2})_3(THF)_2}$ in THF.

VT-NMR Spectra

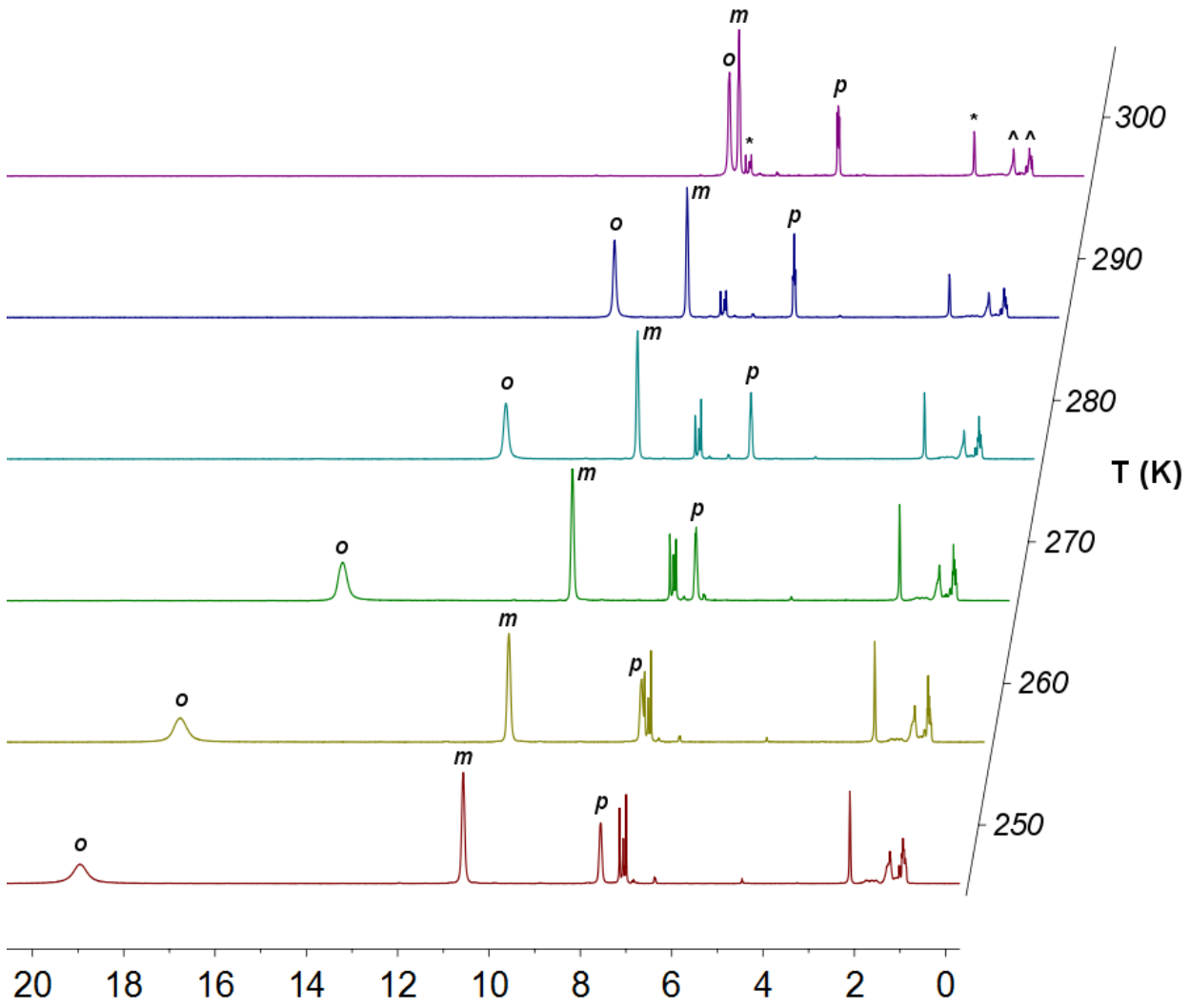

Figure S25. ^{1}H VT NMR data for **U^{IV}(NPh^{F}Ph)$_4$** in toluene-d_8 between 250–300 K. Solvent impurities are marked by * (C_7D_7H) and ^ (hexanes).

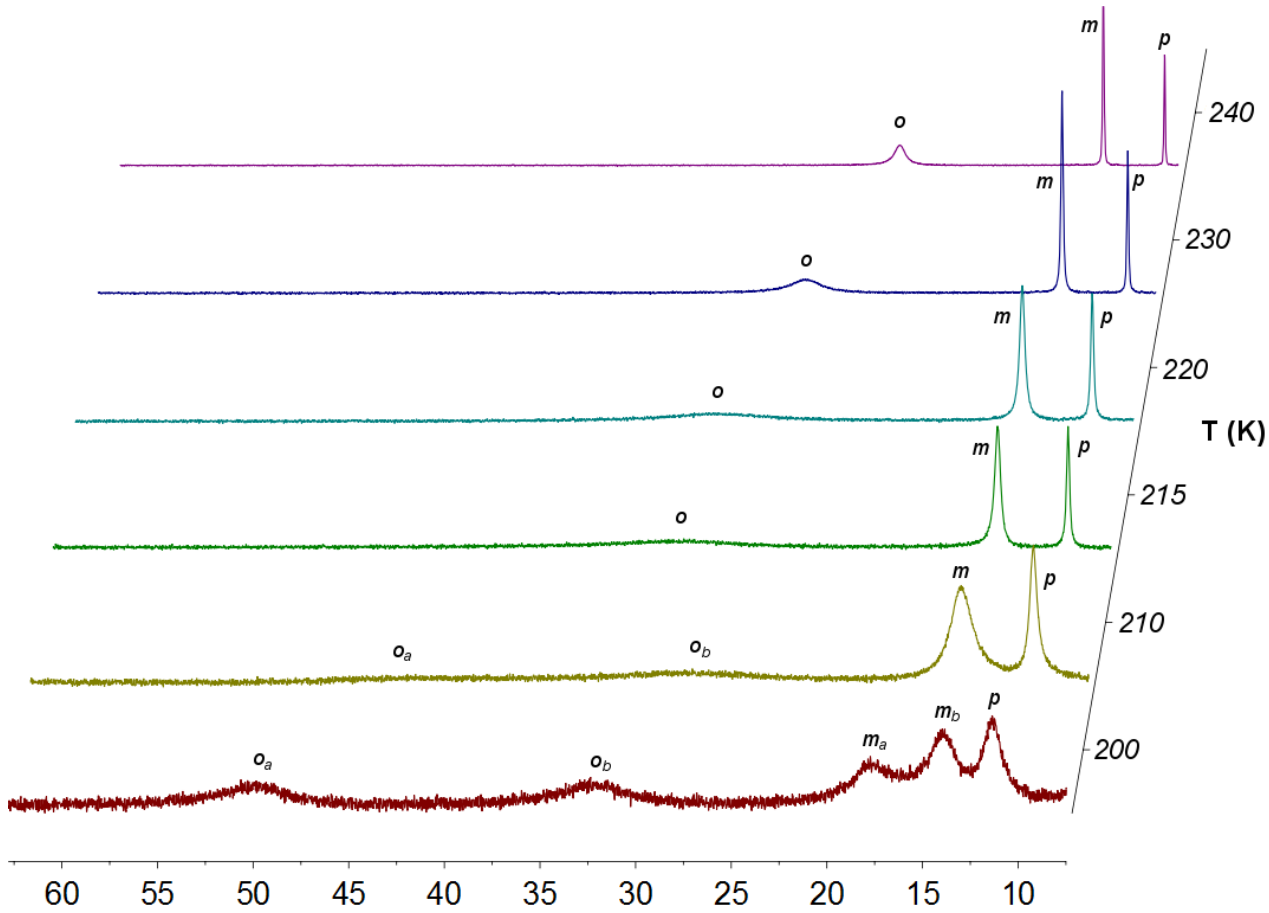

Figure S26. ^{1}H VT NMR data for **U^{IV}(NPh^{F}Ph)$_4$** in toluene-d_8 between 200–250 K. Peaks upfield of 9 ppm were attributed solely to solvent impurities and the presence of trace amounts of HNPh^{F}Ph, so this region of the spectrum was omitted for clarity.

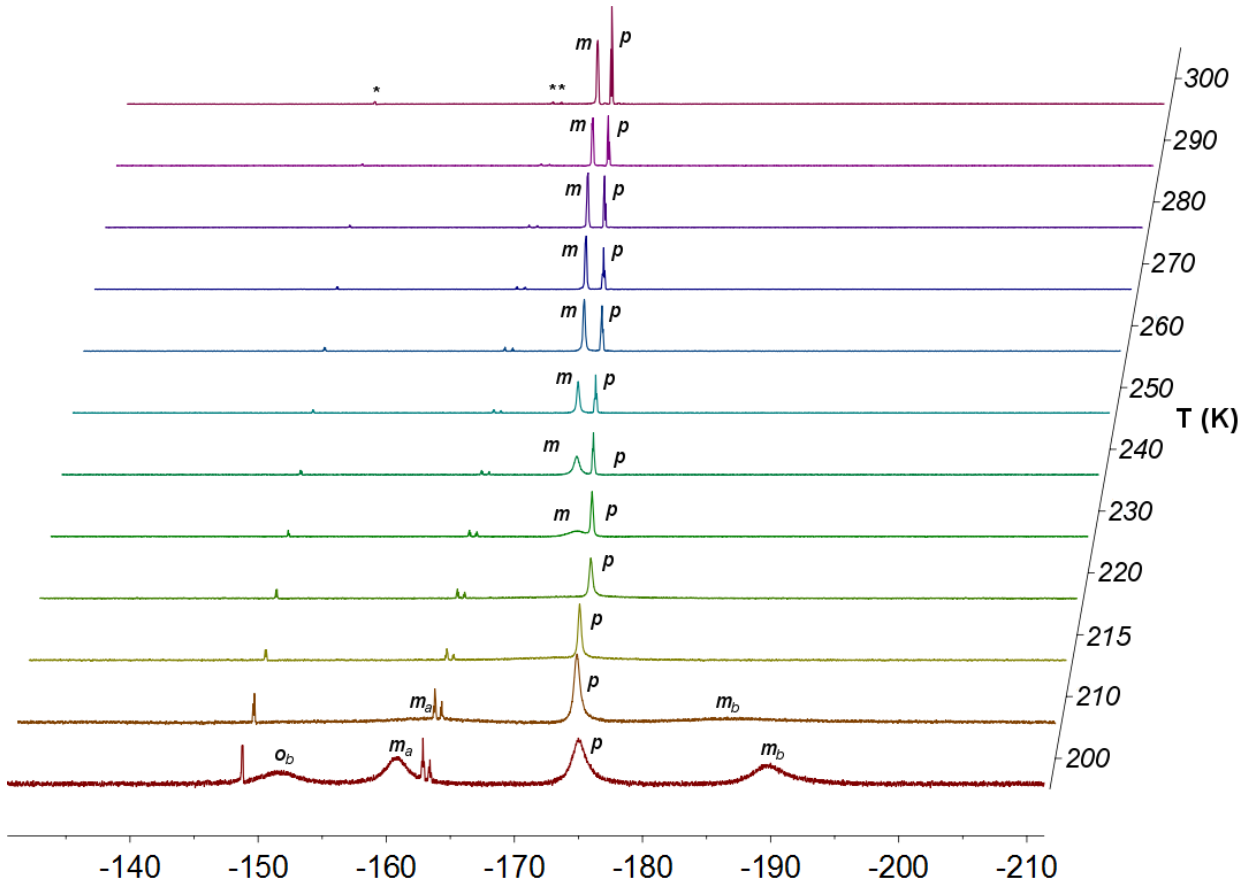

Figure S27. ^{19}F VT NMR data for **U^{IV}(NPh^{F}Ph)$_4$** in toluene-d_8. A minor impurity of HNPh^{F}Ph is visible in all spectra, indicated by *.

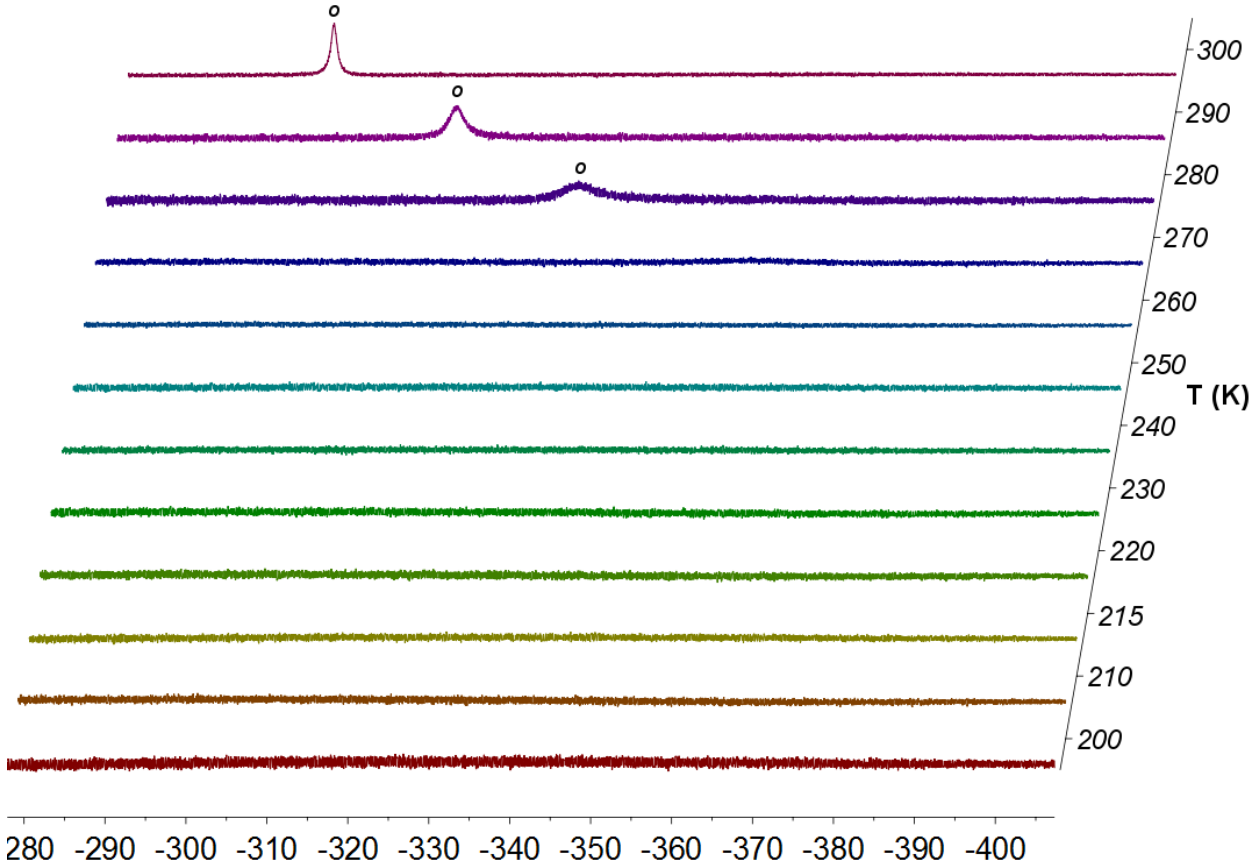

Figure S28. ^{19}F VT NMR data for **U^{IV}(NPh^{F}Ph)$_4$** in toluene-d_8. No peaks were observed upfield of the plotted region at any temperature.

Rotational barrier is calculated according to the equations below.[11]

$$k_c = \frac{\pi}{\sqrt{2}} \Delta\nu_{AB}$$

$$\Delta G^{\neq} = RT ln(\frac{kT}{k_c h})$$

Computational Details

Gaussian 09 Rev. A.02 was used for all electronic structure calculations.[12] The B3LYP hybrid DFT method was employed, with a 60-electron small core pseudopotential on uranium with published segmented natural orbital basis set incorporating quasi-relativistic effects,[13] and the 6-31G* basis set for all other atoms. Geometry optimization on **1–Ph$^{F}_{2}$** was carried out starting from the coordinates of the crystal structure. The only constraint was the spin state (triplet). An optimized geometry in D_2 symmetry was found to have a single imaginary frequency, so a non-symmetric (C_1) geometry was necessary. The frequency calculation indicated that the geometry was the minimum (no imaginary frequencies). Calculated metal-ligand bond lengths were within 0.05 Å of the crystal structure. Molecular orbitals were rendered with the program Chemcraft v1.6,[14] at an isovalue of 0.03. Mayer bond orders and atomic orbital contributions to individual molecular orbitals were calculated with Gaussian with keyword IOp(6/80=1) as well as the AOMix program[15] through fragment molecular orbital analysis. The density of states plot shown in Figure S28 was generated using AOMix.

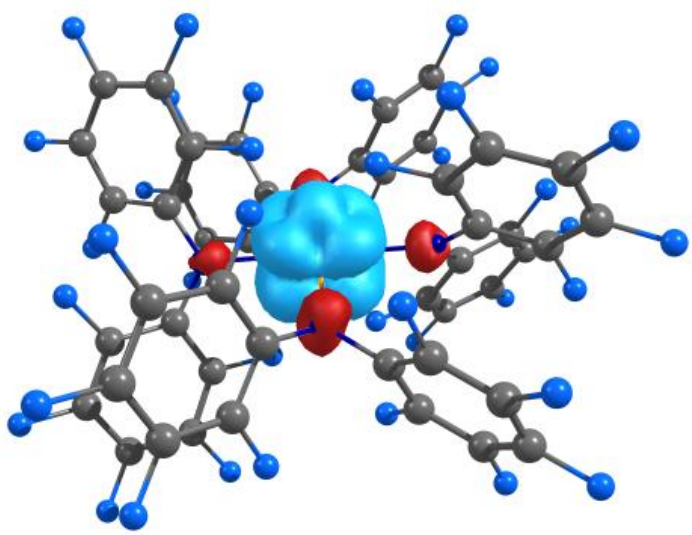

Figure S29. Calculated spin density plot of **U(NPh$^{F}_{2}$)$_4$**.

Table S1. Optimized coordinates for **U(NPh$^{F}_{2}$)$_{4}$**

U	0.000000	0.000000	0.000000	C	-1.129592	-3.093008	0.363685
N	2.400454	0.000000	0.000000	C	-1.740438	-3.968790	-0.548404
N	-2.400454	0.000000	0.000000	C	-2.853509	-4.731298	-0.209394
N	0.000000	2.314054	0.000000	C	-3.400893	-4.626516	1.068641
N	0.000000	-2.314054	0.000000	C	-2.825777	-3.758561	1.994404
C	3.093898	-0.733767	0.966245	C	-1.699126	-3.021943	1.641042
C	2.452407	-0.973480	2.186103	F	1.184667	-0.457893	2.318677
C	2.972826	-1.732265	3.220571	F	2.283912	-1.914567	4.346818
C	4.232930	-2.304747	3.052938	F	4.777743	-3.035716	4.027611
C	4.906407	-2.121253	1.845752	F	6.097320	-2.695900	1.661201
C	4.335340	-1.377600	0.815403	F	4.994844	-1.307719	-0.352521
C	-3.093898	-0.733767	-0.966245	F	-1.184667	-0.457893	-2.318677
C	-2.452407	-0.973480	-2.186103	F	-2.283912	-1.914567	-4.346818
C	-2.972826	-1.732265	-3.220571	F	-4.777743	-3.035716	-4.027611
C	-4.232930	-2.304747	-3.052938	F	-6.097320	-2.695900	-1.661201
C	-4.906407	-2.121253	-1.845752	F	-4.994844	-1.307719	0.352521
C	-4.335340	-1.377600	-0.815403	F	1.256283	4.062594	-1.797517
C	1.129592	3.093008	0.363685	F	3.417579	5.539033	-1.112939
C	1.740438	3.968790	-0.548404	F	4.476876	5.342734	1.397920
C	2.853509	4.731298	-0.209394	F	3.343232	3.651217	3.221367
C	3.400893	4.626516	1.068641	F	1.156561	2.205112	2.559445
C	2.825777	3.758561	1.994404	F	-1.256283	4.062594	1.797517
C	1.699126	3.021943	1.641042	F	-3.417579	5.539033	1.112939
C	-1.129592	3.093008	-0.363685	F	-4.476876	5.342734	-1.397920
C	-1.740438	3.968790	0.548404	F	-3.343232	3.651217	-3.221367
C	-2.853509	4.731298	0.209394	F	-1.156561	2.205112	-2.559445
C	-3.400893	4.626516	-1.068641	F	1.184667	0.457893	-2.318677
C	-2.825777	3.758561	-1.994404	F	2.283912	1.914567	-4.346818
C	-1.699126	3.021943	-1.641042	F	4.777743	3.035716	-4.027611
C	3.093898	0.733767	-0.966245	F	6.097320	2.695900	-1.661201
C	2.452407	0.973480	-2.186103	F	4.994844	1.307719	0.352521
C	2.972826	1.732265	-3.220571	F	-1.184667	0.457893	2.318677
C	4.232930	2.304747	-3.052938	F	-2.283912	1.914567	4.346818
C	4.906407	2.121253	-1.845752	F	-4.777743	3.035716	4.027611
C	4.335340	1.377600	-0.815403	F	-6.097320	2.695900	1.661201
C	-3.093898	0.733767	0.966245	F	-4.994844	1.307719	-0.352521
C	-2.452407	0.973480	2.186103	F	1.256283	-4.062594	1.797517
C	-2.972826	1.732265	3.220571	F	3.417579	-5.539033	1.112939
C	-4.232930	2.304747	3.052938	F	4.476876	-5.342734	-1.397920
C	-4.906407	2.121253	1.845752	F	3.343232	-3.651217	-3.221367
C	-4.335340	1.377600	0.815403	F	1.156561	-2.205112	-2.559445
C	1.129592	-3.093008	-0.363685	F	-1.256283	-4.062594	-1.797517
C	1.740438	-3.968790	0.548404	F	-3.417579	-5.539033	-1.112939
C	2.853509	-4.731298	0.209394	F	-4.476876	-5.342734	1.397920
C	3.400893	-4.626516	-1.068641	F	-3.343232	-3.651217	3.221367
C	2.825777	-3.758561	-1.994404	F	-1.156561	-2.205112	2.559445
C	1.699126	-3.021943	-1.641042				

Table S2. Comparison of parameters between X-ray structure and optimized model for **U(NPh$^F_2$)$_4$**

	X-ray structure	Optimized model	Difference
U-N$_{average}$	2.328(2)	2.357	0.029
U-F$_{average}$ [a]	2.6233(13)	2.6437	0.020
N-U-N$_{average}$	90.00(6)	90.00	0.00
F-U-F [b]	126.87(5)	126.76	0.11

[a] Considering only U-F short contacts. [b] Both U-F short contacts originate from the same NPh$^F_2$ ligand.

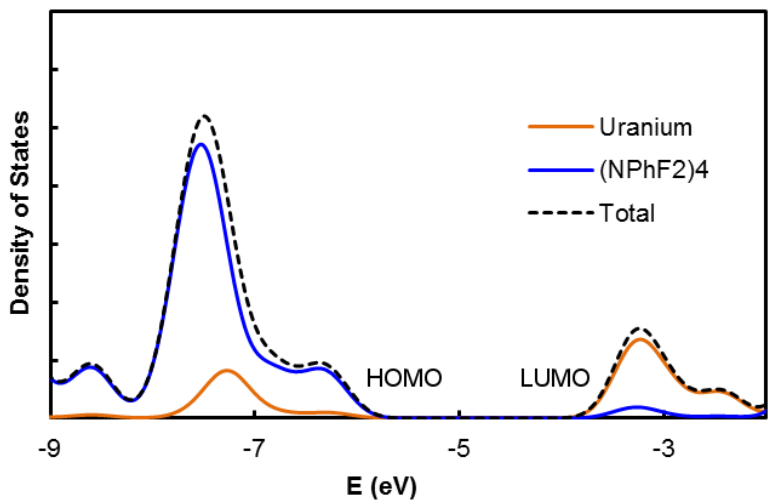

Figure S30. Density of alpha spin states plot for **1-Ph$^F_2$** around the HOMO-LUMO gap, showing relative contribution of metal- and ligand-based orbitals to the full molecular orbitals.

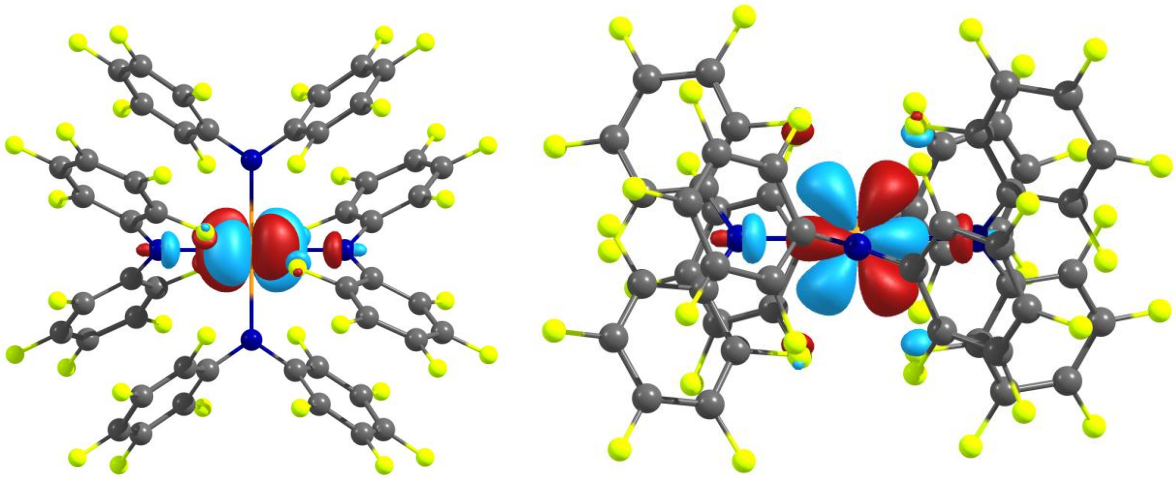

Figure S31. LUMO+4 of **1-Ph$^F_2$** viewed from the top (left) and side (right). This molecular orbital contains 91.7% U(5f) AO character.

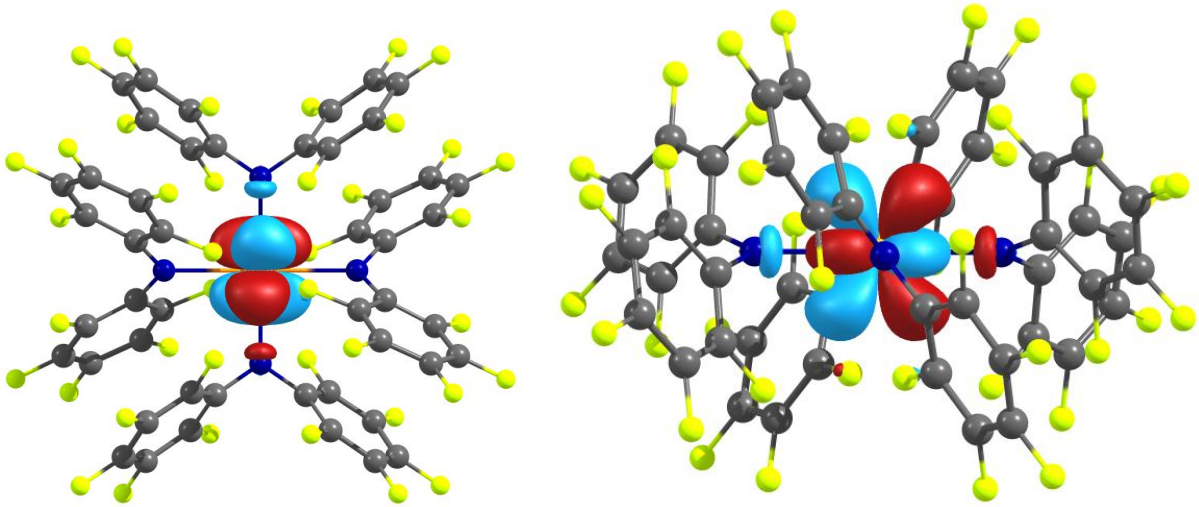

Figure S32. LUMO+3 of **1-Ph$^F_2$** viewed from the top (left) and side (right). This molecular orbital contains 93.5% U(5f) AO character.

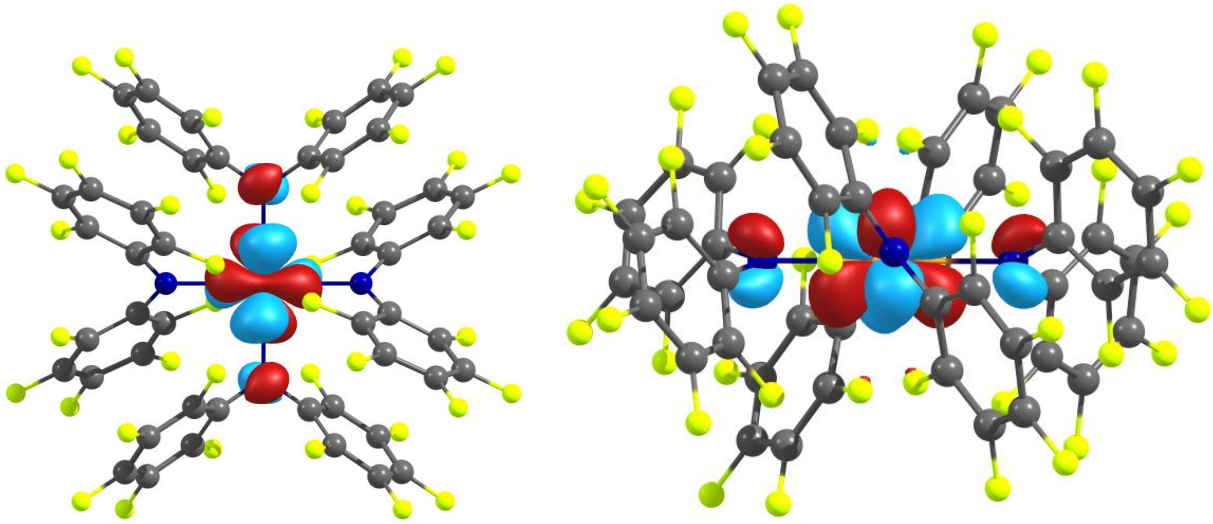

Figure S33. LUMO+2 of **1-Ph$^F_2$** viewed from the top (left) and side (right). This molecular orbital contains 88.1% U(5f) AO character.

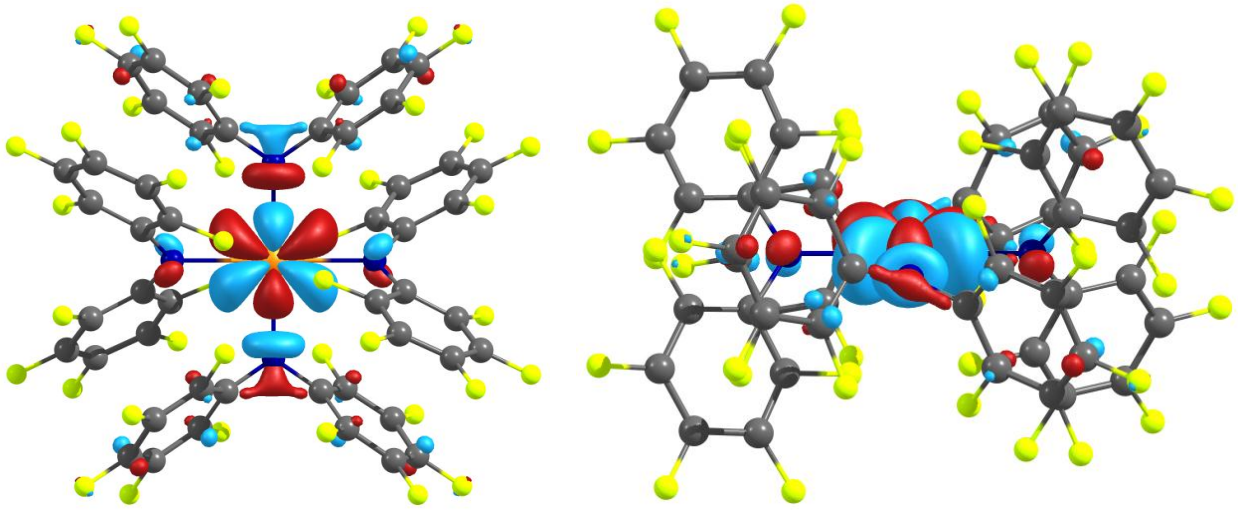

Figure S34. LUMO+1 of **1-Ph$^{F}_{2}$** viewed from the top (left) and side (right). This molecular orbital contains 78.8% U(5f) AO character.

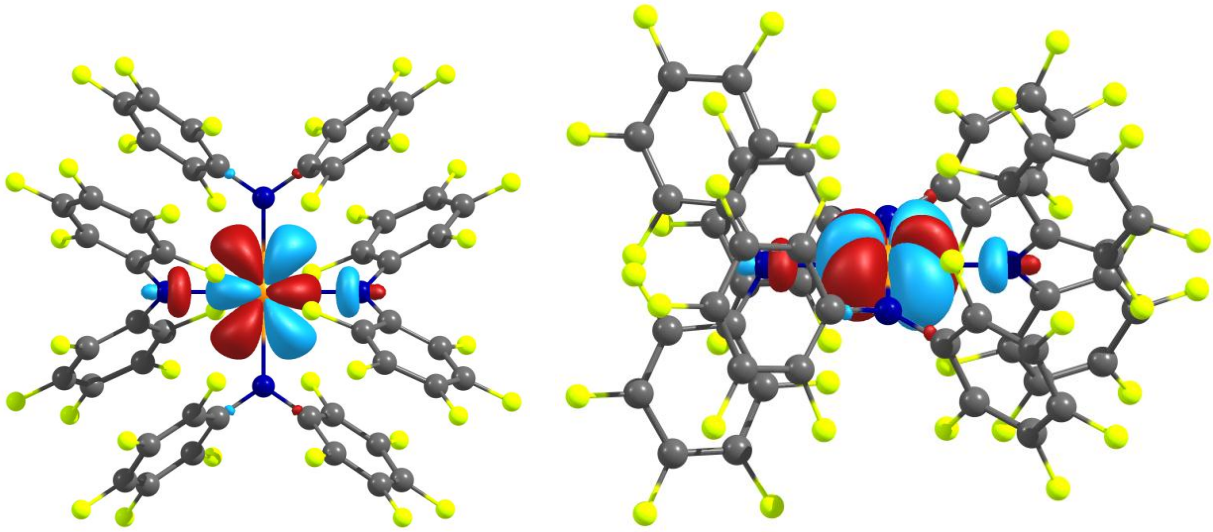

Figure S35. LUMO of **1-Ph$^{F}_{2}$** viewed from the top (left) and side (right). This molecular orbital contains 89.5% U(5f) AO character.

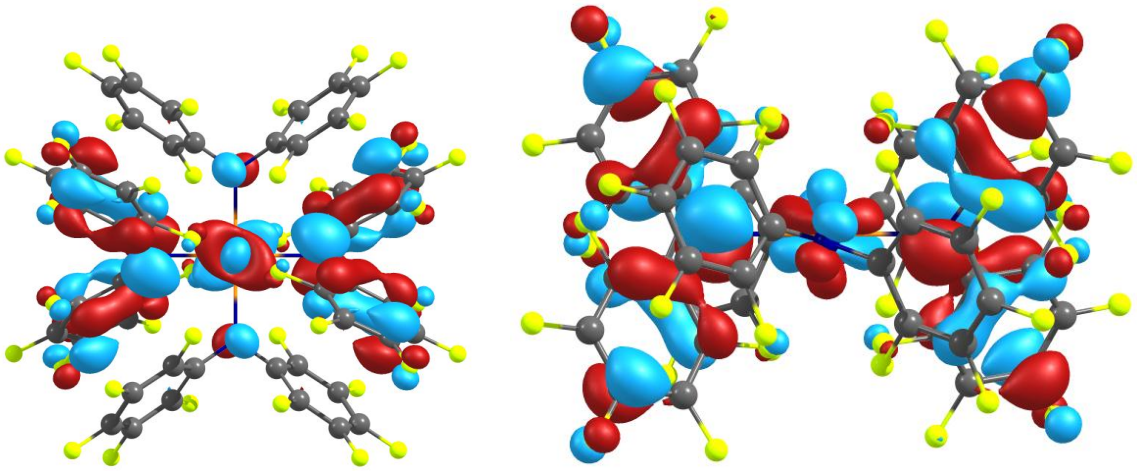

Figure S36. HOMO of **1-Ph$^{F}_{2}$** viewed from the top (left) and side (right). This molecular orbital contains 13.8% U(5f) AO character.

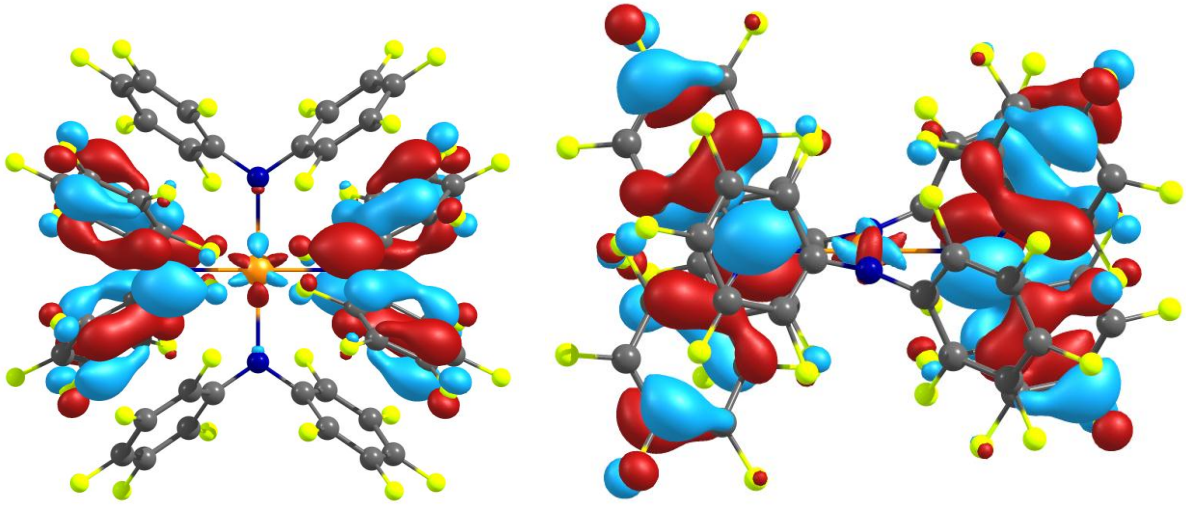

Figure S37. HOMO–1 of **1-Ph$^{F}_{2}$** viewed from the top (left) and side (right). This molecular orbital contains 1.8% U(5f) AO character.

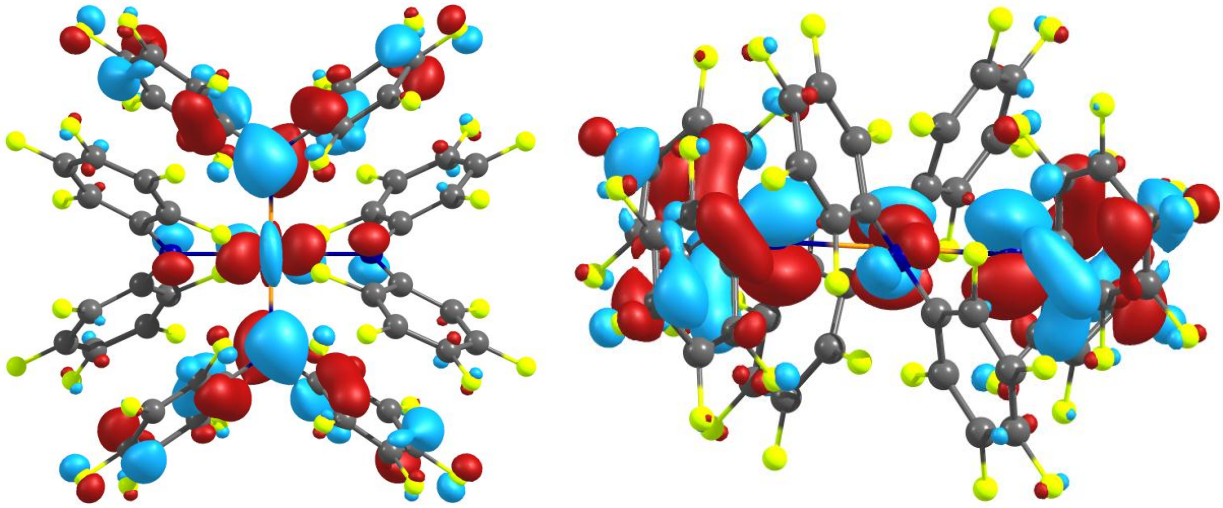

Figure S38. HOMO–2 of **1-Ph$^F_2$** viewed from the top (left) and side (right). This molecular orbital contains 15.1% U(5f) AO character.

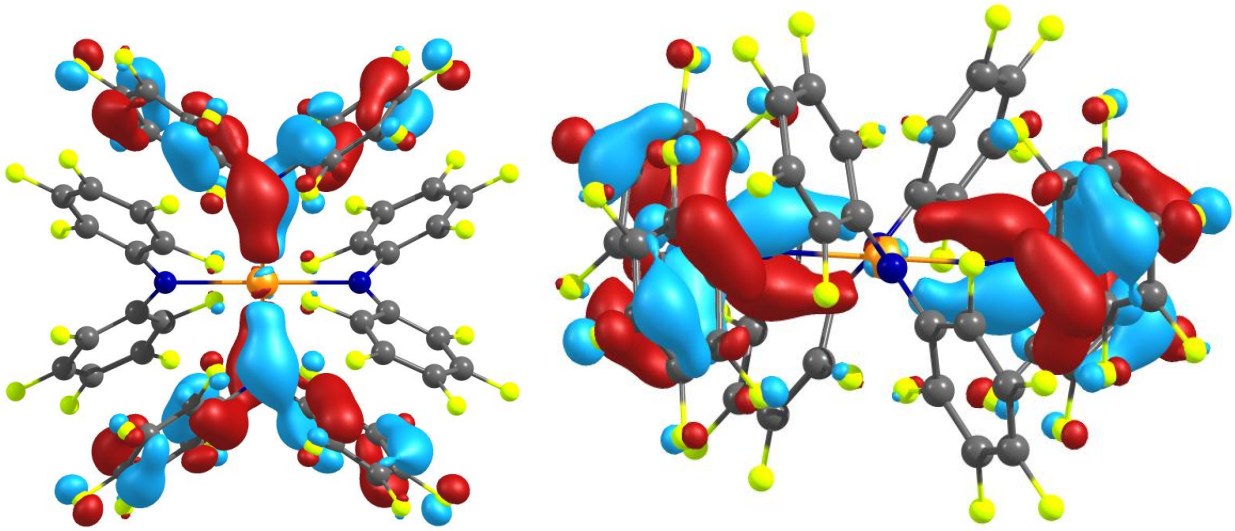

Figure S39. HOMO–3 of **1-Ph$^F_2$** viewed from the top (left) and side (right). This molecular orbital contains 0.2% U(5f) AO character.

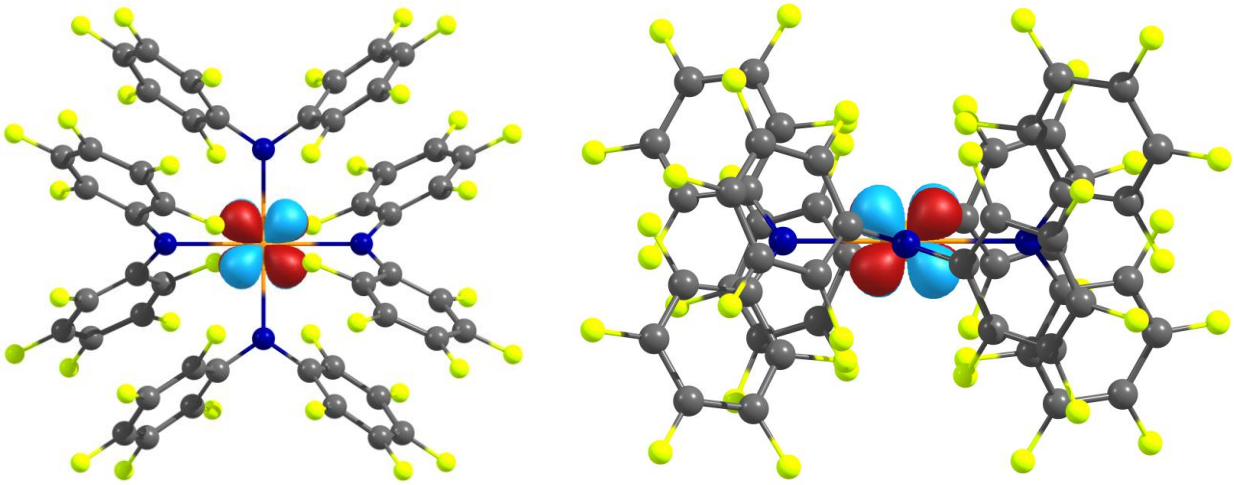

Figure S40. HOMO-4 of **1-Ph$^F_2$** viewed from the top (left) and side (right). This molecular orbital contains 95.0% U(5f) AO character.

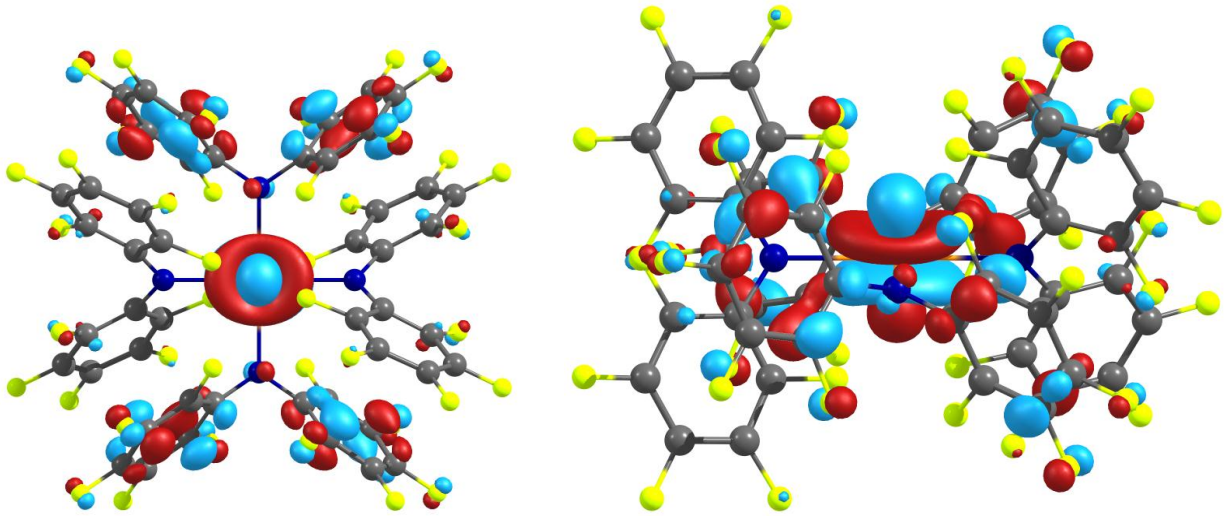

Figure S41. HOMO-5 of **1-Ph$^F_2$** viewed from the top (left) and side (right). This molecular orbital contains 57.2% U(5f) AO character.

Deconvolution of electronic absorption spectra

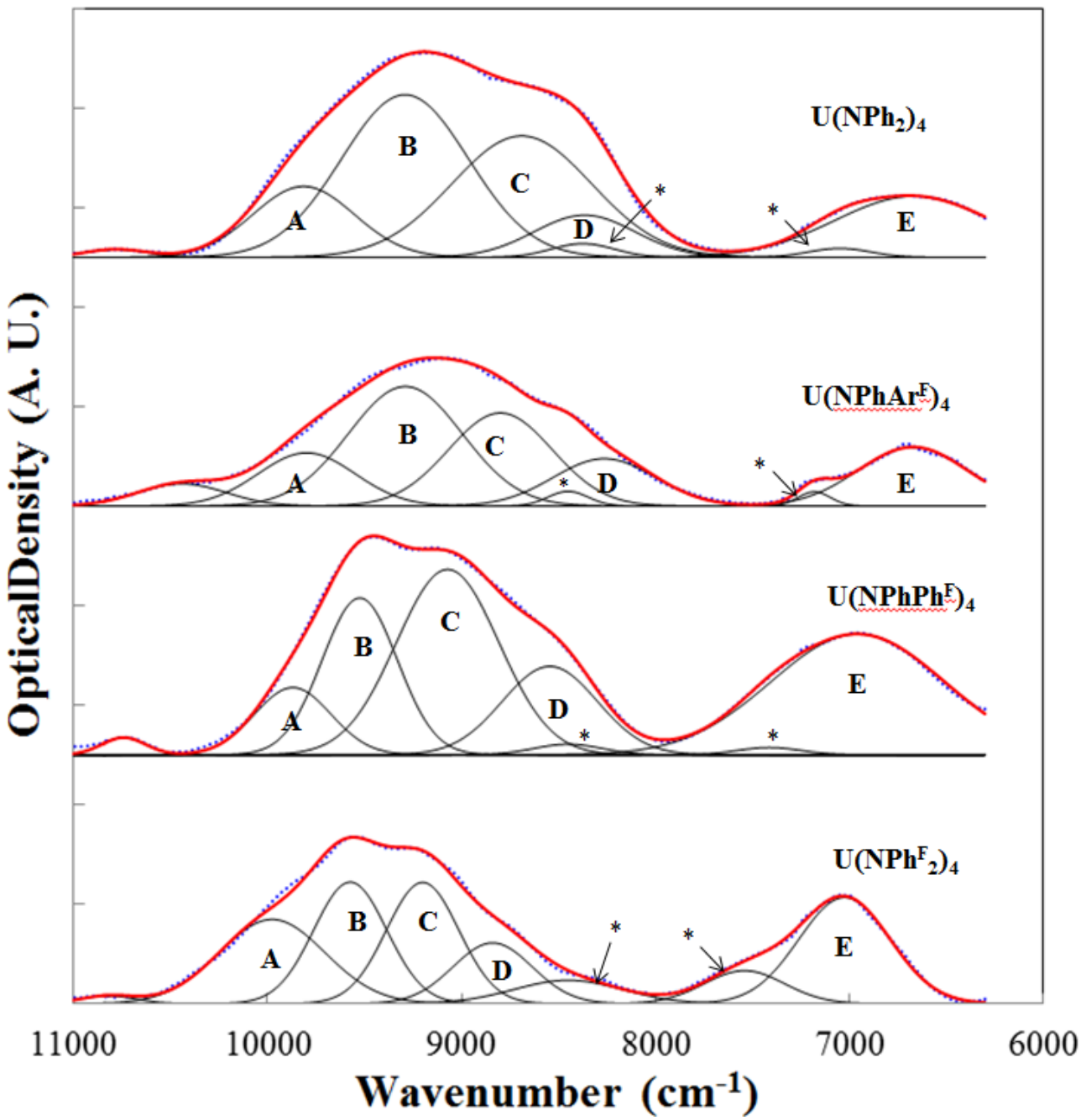

Fig. S42. Spectral deconvolutions of near-IR region of electronic spectra for **U(NPhAr^F)$_4$, U(NPh$_2$)$_4$, U(NPh$^F{}_2$)$_4$, U(NPhPh^F)$_4$** (from top to bottom) in a fluorobenzene solution at room temperature. Spectra are offset for clarity. Experimental data (blue dash line) are fit with Gaussian bands (black solid line). The sum is presented in red solid line. The asterisk denotes the small contribution from solvent vibrational band that was incompletely subtracted. Labels on each component fit bands correspond to those listed in **Table S3**.

Table S3. Summary of electronic spectral data for **U(NAr$_2$)$_4$** complexes in a fluorobenzene solution at room temperature. The oscillator strength of **E** bands is arbitrary set as 10 and the relative oscillator strength of bands **A** to **D** are calculated accordingly.

Complex	f→f electronic transition (E) and relative oscillator strength (*f*)									
	A		**B**		**C**		**D**		**E**	
	E (cm^{-1})	*f*	E (cm^{-1})	*f*	E (cm^{-1})	*f*	E (cm^{-1})	*f*	E (cm^{-1})	*f*
U(NPhPh^F)$_4$ (1-PhPh^F)	9869	2.4	9524	5.6	9071	9.1	8544	4.0	6956	10
U(NPh$^F_2$)$_4$ (1-Ph$^F_2$)	9976	9.2	9573	9.2	9200	9.1	8839	2.6	7025	10
U(NPh$_2$)$_4$ (1-Ph$_2$)	9813	7.4	9290	21	8689	18	8365	4.4	6668	10
U(NPhAr^F)$_4$ (1-PhAr^F)	9798	8.0	9289	21	8799	15	8263	7.5	6673	10

References:

1. M. Wojdyr, *J. Appl. Crystallogr.*, 2010, **43**, 1126-1128.
2. C. D. Carmichael, N. A. Jones and P. L. Arnold, *Inorg. Chem.*, 2008, **47**, 8577-8579.
3. R. Koppang, *Acta Chem. Scand.*, 1971, **25**, 3067-3071.
4. R. Poe, K. Schnapp, M. J. T. Young, J. Grayzar and M. S. Platz, *J. Am. Chem. Soc.*, 1992, **114**, 5054-5067.
5. Bruker (2009) SAINT. Bruker AXS Inc., Madison, Wisconsin, USA.
6. Bruker (2009) SHELXTL. Bruker AXS Inc., Madison, Wisconsin, USA.
7. Sheldrick, G.M. (2008) TWINABS. University of Gottingen, Germany.
8. Sheldrick, G.M. (2007) SADABS. University of Gottingen, Germany.
9. Sheldrick, G.M. (2008) Acta Cryst. A64,112-122.
10. J. G. Reynolds, A. Zalkin, D. H. Templeton and N. M. Edelstein, *Inorg. Chem.*, 1977, **16**, 1090-1096.
11. H. Friebolin, *Basic One- and Two-Dimensional NMR Spectroscopy*, Wiley, 2005.
12. Gaussian 09, Revision A.02, M. J. Frisch, G. W. Trucks, H. B. Schlegel, G. E. Scuseria, M. A. Robb, J. R. Cheeseman, G. Scalmani, V. Barone, B. Mennucci, G. A. Petersson, H. Nakatsuji, M. Caricato, X. Li, H. P. Hratchian, A. F. Izmaylov, J. Bloino, G. Zheng, J. L. Sonnenberg, M. Hada, M. Ehara, K. Toyota, R. Fukuda, J. Hasegawa, M. Ishida, T. Nakajima, Y. Honda, O. Kitao, H. Nakai, T. Vreven, J. A. Montgomery, Jr., J. E. Peralta, F. Ogliaro, M. Bearpark, J. J. Heyd, E. Brothers, K. N. Kudin, V. N. Staroverov, R. Kobayashi, J. Normand, K. Raghavachari, A. Rendell, J. C. Burant, S. S. Iyengar, J. Tomasi, M. Cossi, N. Rega, J. M. Millam, M. Klene, J. E. Knox, J. B. Cross, V. Bakken, C. Adamo, J. Jaramillo, R. Gomperts, R. E. Stratmann, O. Yazyev, A. J. Austin, R. Cammi, C. Pomelli, J. W. Ochterski, R. L. Martin, K. Morokuma, V. G. Zakrzewski, G. A. Voth, P. Salvador, J. J. Dannenberg, S. Dapprich, A. D. Daniels, O. Farkas, J. B. Foresman, J. V. Ortiz, J. Cioslowski, and D. J. Fox, Gaussian, Inc., Wallingford CT, 2009.
13. (a) Institute for Theoretical Chemistry, University of Cologne, http://www.tc.unikoeln.de/PP/clickpse.en.html (b) W. Kuechle, M. Dolg, H. Stoll, H. Preuss J. Chem. Phys. 100, 7535 (1994). (c) X. Cao, M. Dolg, H. Stoll, J. Chem. Phys. 118, 487 (2003) (c) X. Cao, M. Dolg, J. Molec. Struct. (Theochem) 673, 203 (2004)
14. http://www.chemcraftprog.com/.
15. (a) S. I. Gorelsky, AOMix: Program for Molecular Orbital Analysis, http://www.sgchem.net/, University of Ottawa, version 6.5, 2011. (b) S. I. Gorelsky, A. B. P. Lever, J. Organomet. Chem. 2001, 635, 187–196.